DEVELOPMENT OF AN ELECTRO-MAGNETIC VALVE ACTUATION SYSTEM ON A KOHLER ENGINE

FINAL INTERIM REPORT
TFLRF No. 327

By
Daniel J. Podnar
U.S. Army TARDEC Fuels and Lubricants Research Facility
Southwest Research Institute
San Antonio, Texas

prepared for

Defense Advanced Research Projects Agency
3701 N. Fairfax Drive
Arlington, Virginia 22203-1714

Under Contract to
U.S. Army TARDEC
Petroleum and Water Business Area
Warren, Michigan 58397

Contract No. DAAK70-92-C-0059

Approved for public release; distribution unlimited

March 1998

Disclaimers

The findings in this report are not to be construed as an official Department of the Army position unless so designated by other authorized documents.

Trade names cited in this report do not constitute an official endorsement or approval of the use of such commercial hardware or software.

DTIC Availability Notice

Qualified requestors may obtain copies of this report from the Defense Technical Information Center, Attn: DTIC-OCC, 8725 John J. Kingman Road, Suite 0944, Fort Belvoir, Virginia 22060-6218.

Disposition Instructions

Destroy this report when no longer needed. Do not return it to the originator.

REPORT DOCUMENTATION PAGE

Form Approved
OMB No. 0704-0188

1. AGENCY USE ONLY (Leave blank)	2. REPORT DATE	3. REPORT TYPE AND DATES COVERED
	March 1998	Interim December 1994 – May 1997

4. TITLE AND SUBTITLE

Development of a Natural Gas-Powered APU for a Hybrid Electric S-10 Pickup Truck

5. FUNDING NUMBERS

DAAK70-92-C-0059;
WD 20,36

6. AUTHOR(S)

Podnar, Daniel J.

7. PERFORMING ORGANIZATION NAME(S) AND ADDRESS(ES)

U.S. Army TARDEC Fuels and Lubricants Research Facility (SwRI)
Southwest Research Institute
P.O. Drawer 28510
San Antonio, Texas 78228-0510

8. PERFORMING ORGANIZATION REPORT NUMBER

TFLRF No. 327

9. SPONSORING/MONITORING AGENCY NAME(S) AND ADDRESS(ES)

U. S. Army TARDEC
Petroleum and Water Business Area
Warren, Michigan 58397-5000

10. SPONSORING/MONITORING AGENCY REPORT NUMBER

11. SUPPLEMENTARY NOTES

12a. DISTRIBUTION/AVAILABILITY STATEMENT

Approved for public release; distribution unlimited

12b. DISTRIBUTION CODE

13. ABSTRACT (Maximum 200 words)

An electromagnetic valve actuation (EVA) system was developed and applied to a Kohler Command Series engine. The EVA system was developed for the Kohler engine by Aura Systems of El Segundo CA. Southwest Research Institute (SwRI) was responsible for evaluating the performance of the EVA equipped engine, running on natural gas, in a laboratory test environment. As part of this effort, SwRI applied a personal computer-based engine control system which managed the fueling, ignition, throttling, and intake/exhaust valve control functions. Advantages from utilizing the EVA system on the engine proved to be increased engine power and full load efficiency at low speed operation, and increased part load efficiency at all engine speeds.

14. SUBJECT TERMS

variable valve timing
natural gas engine
compressed natural gas
Miller Cycle operation
electro-magnetic valve actuation
electronic engine control
throttleless engine operation

15. NUMBER OF PAGES

51

16. PRICE CODE

17. SECURITY CLASSIFICATION OF REPORT	18. SECURITY CLASSIFICATION OF THIS PAGE	19. SECURITY CLASSIFICATION OF ABSTRACT	20. LIMITATION OF ABSTRACT
Unclassified	Unclassified	Unclassified	

EXECUTIVE SUMMARY

The purpose of this project was to develop and demonstrate an electro-magnetic valve actuation (EVA) system on a Kohler engine. A custom application of the EVA system, developed by Aura Systems of El Segundo, CA, was adapted for use on a Kohler Command series utility engine. The stock gasoline-powered Kohler engine was converted to operate on compressed natural gas (CNG), and a prototype engine/valve control system was developed and applied by Southwest Research Institute (SwRI). The engine system was subsequently evaluated in the engine test laboratory environment to demonstrate the benefits of using the computer-controlled variable valve timing system. Engine operation was tested with the following three strategies:

- Throttled operation with engine speed optimized valve events
- Optimized unthrottled operation utilizing early intake valve closing (EIVC) for load modulation
- Optimized unthrottled operation utilizing late intake valve closing (LIVC) for load modulation

The results of the engine testing indicated three (3) significant advantages of the EVA-equipped engine, as compared to a similarly equipped engine using a conventional cam-driven valve train. The advantages include the following:

- Increased full load torque and power over the lower speed portion of the operating range
- Increased full load efficiency over the lower speed portion of the operating range
- Increased part load efficiency using the unthrottled EIVC or LIVC approaches

TABLE OF CONTENTS

LIST OF ILLUSTRATIONS

Figure **Page**

LIST OF ILLUSTRATIONS

Table **Page**

1.0 BACKGROUND

1.1 Objective

The technical objective of the project was to modify, integrate, and test an electro-magnetic valve actuation (EVA) system on a Kohler Command series utility engine. The process and results of this effort are documented within the Technical Discussion portion of this report.

1.2 Technical Background

SwRI has developed an auxiliary power unit (APU) for a hybrid electric S-10 pickup truck. The APU for that vehicle utilized a highly modified Kohler Command series engine, which SwRI developed to operate on natural gas. As a result of this effort, a wealth of engine performance data and technical information was accumulated for the modified version of the Kohler engine. The original interest in Aura Systems' EVA system was to ultimately apply an EVA-equipped Kohler engine in the vehicle for field demonstration. Due to funding and schedule reasons, the project objectives were changed to include only laboratory development and evaluation of the EVA-equipped engine.

Aura Systems' EVA system was selected as a candidate technology due to its technical attributes. The system was developed as a computer-controlled valve actuation system with a fast response, efficient actuator and servo control system design. The benefits of a variable valve timing (VVT) system are well documented in the literature, with potential for improvements in engine power and efficiency, as well as emissions. However, most VVT systems do not provide complete flexibility in control of each valve event for each intake and exhaust valve on an engine. The EVA system provides this capability.

2.0 TECHNICAL DISCUSSION

The Technical Discussion section of this report details the technical work performed on the project, as well as the performance data generated and conclusions drawn from the data.

2.1 EVA Overview

Aura Systems' EVA system is made up of eight fundamental parts for each actuator: two electromagnets, two opposing springs, an armature, an armature guidance mechanism, a valve, and a valve guidance mechanism. The two electromagnets (one providing force to open the valve, the other to close the valve) provide supplemental forces to control the position of the armature, and hence the valve. The primary forces acting on the valve, however, are provided by the two spring coils located on either side of the armature. The basic EVA concept is illustrated in Figure 1.

From an unpowered condition, the equilibrium position of the valve is partially open. Once electrical power is provided, the appropriate electromagnet is energized to provide the force needed to act against the springs and produce the desired valve motion (the open or closed position). Subsequent valve transitions are initiated by de-energizing the appropriate electromagnet. The spring coils then provide the force for transitioning the valve through the equilibrium position and toward the new desired position. Only when the valve position nears the new desired position is the electromagnet associated with the new position energized to provide the force needed to complete the transition at the desired seating velocity. With this concept, the required size and power consumption of the electromagnets are minimized. However, the control electronics required to reliably complete each valve transition and achieve "soft landings" becomes complicated. More detailed information on the EVA system is contained in Appendix A.

2.2 EVA Application to Kohler Engine

SwRI supplied a stock Kohler CH-18 gasoline engine to Aura Systems to be outfitted with a customized version of the EVA system. Aura Systems performed this work from December 1994 to October 1996. The final configuration of the EVA system on the Kohler engine was named a Valve Outside Rotating Armature Design (VORAD). This configuration, which features an armature that moves rotationally and is offset from the valve stem, is illustrated in Figure 2. A detailed description of the engineering effort conducted by Aura Systems is contained in Appendix A.

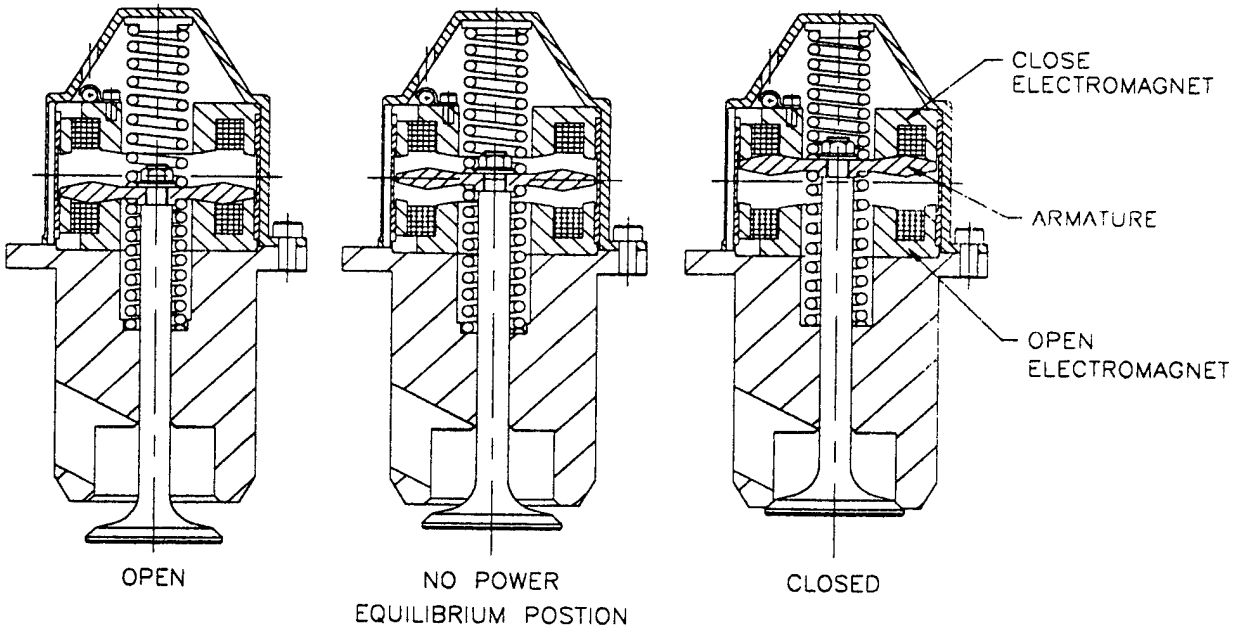

Figure 1. Basic EVA Concept

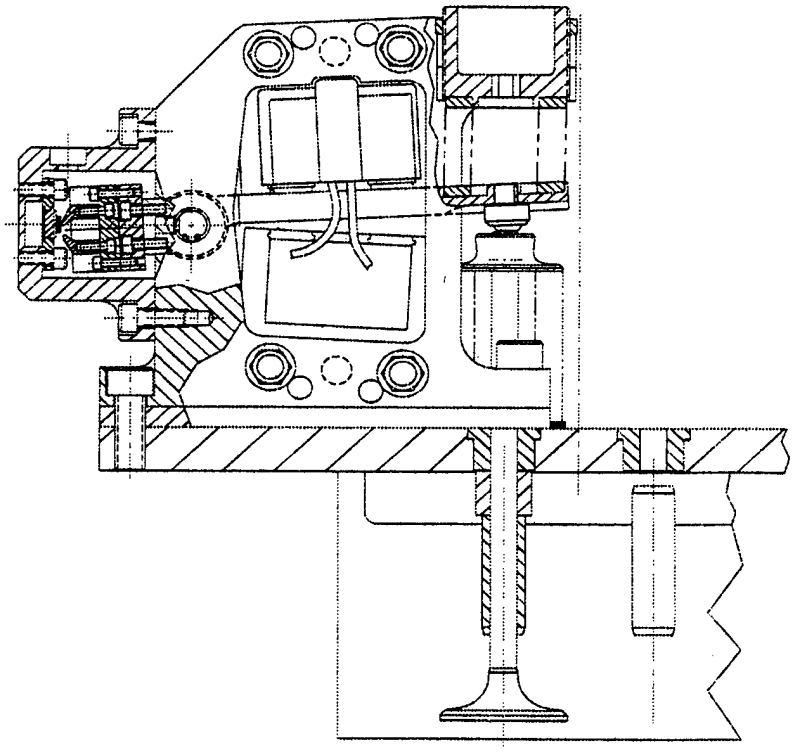

Figure 2. VORAD Actuator and Cylinder Head Layout

2.3 SwRI Engine/Valve Control System

The electronics package for control of the EVA system, as shipped from Aura Systems, consisted of a servo controller and Engine Control Unit (ECU). The servo controller served the purpose of controlling the power to the electromagnets based on the valve open/close command signal from the ECU and the position feedback from the Hall Effect sensors. The servo controller was developed by Aura Systems and was an integral part of the EVA system. The ECU was responsible for generating valve open/close command signals for use by the servo controller (based on crank angle position and intake manifold pressure inputs). The ECU was developed by BKM of San Diego, CA. The ECU was not an integral part of the EVA system and could be replaced with any suitable control unit capable of generating the appropriate 0-to-5V command signals for the servo controller. Since the stock Kohler engine did not provide electronic control of fuel delivery or spark timing, it was decided that an electronic engine control system, similar in function to the one used on the Kohler APU engine development effort, would be applied for the project. In addition, since the BKM ECU provided a cumbersome user interface and would represent a third control system on the overall engine system, it was decided that SwRI would apply a single prototype controller to combine the functions of the BKM ECU and the engine control system. A customized version of SwRI's Rapid Prototyping Engine Control System (RPECS) was assembled and applied to the Kohler engine. The RPECS was interfaced with the Aura Systems servo controller to provide independent control over each valve event for each of the two intake and exhaust valves on the engine. A photograph of the electronic controllers, i.e. the SwRI RPECS and the Aura Systems servo controller, is shown in Figure 3.

The RPECS provided closed loop adaptive control of engine fueling, control of the spark timing and coil dwell functions, control of a "drive-by-wire" throttle actuator, and control of valve open and close angles for each valve. The valve open and close angle values were determined from lookup tables (or maps) with independent variables of either manifold absolute pressure (MAP) or operator demand (analogous to pedal position), and engine speed. The selection of the first independent variable was based on whether throttled or unthrottled operation was desired. A typical valve event map is shown in Figure 4.

Figure 3. EVA Engine Control Electronics

KOHLER EVA CONTROLLER - INTAKE VALVE EVENT MAP

Engine Speed (RPM)

IND VAR %	800	1200	1600	2000	2200	2400	2600	2800	3200	3600	3800	4000
0.0	19	22	29	36	38	40	41	43	50	59	64	69
	202	179	178	180	182	184	186	189	197	202	205	208
20.0	19	22	29	36	38	40	41	43	50	59	64	69
	202	179	178	180	182	184	186	189	197	202	205	208
40.0	19	22	29	36	38	40	41	43	50	59	64	69
	202	179	178	180	182	184	186	189	197	202	205	208
60.0	19	22	29	36	38	40	41	43	50	59	64	69
	202	179	178	180	182	184	186	189	197	202	205	208
70.0	19	22	29	36	38	40	41	43	50	59	64	69
	202	179	178	180	182	184	186	189	197	202	205	208
80.0	19	22	29	36	38	40	41	43	50	59	64	69
	202	179	178	180	182	184	186	189	197	202	205	208
90.0	19	22	29	36	38	40	41	43	50	59	64	69
	202	179	178	180	182	184	186	189	197	202	205	208
100.0	19	22	29	36	38	40	41	43	50	59	64	69
	202	179	178	180	182	184	186	189	197	202	205	208

Speed	0 rpm	Int_Open	19.0 CAD	MAP	1.6 psia
MAPBar	11.0 %Bar	Int_Cls	202.0 CAD	RunMode	STOPPED
EGO	0.205 volts	ThrotCmd	0.1 Volts	RunTime	00:00:00

Figure 4. Typical Valve Event Map

2.4 Engine Conversion to CNG Operation

As previously noted, a stock gasoline-powered Kohler CH-18 engine was outfitted with the EVA system. Since the stock engine is carbureted and ignition timing is fixed, and since a wealth of engine data was gathered with the CNG engine on the APU development project, it was decided that the EVA engine would be converted to CNG operation and an electronic engine control system would be applied. This would allow for a direct comparison of the EVA engine to the final engine from the APU development project.

The engine modifications made in the conversion process included piston and connecting rod replacement, removal of the stock carburetor in favor of the fuel injection system, replacement of the exhaust system, replacement of the ignition system, and replacement of the throttle body. Piston replacement was necessary to increase compression ratio to that of the APU development engine (12:1). Similarly, an upgraded connecting rod, designed by SwRI during the APU development project, was used. This was necessary since failures of the stock connecting rods were experienced in the APU development project due to the increased loads from the higher compression ratio. As previously mentioned, an electronic engine control system was applied to the engine, enabling the removal of the stock carburetor and ignition system. Also, a custom exhaust header system replaced the stock exhaust system. The header system was developed

during the APU development project and improved the breathing characteristics of the engine. Finally, the stock throttle body was replaced with an enlarged throttle body that had been fabricated at SwRI during the previous project. Upon making these changes, the EVA engine was configured similarly to the final engine from the APU development project. Once the engine modifications were completed, the engine was installed in an engine test cell at SwRI and coupled to an eddy current dynamometer. The EVA engine, as installed in the engine test laboratory, is shown in Figure 5.

2.5 Engine Testing

The EVA-equipped engine was tested in both the gasoline and CNG configurations. The engine was tested briefly during the EVA application task by Aura Systems, and was extensively tested by SwRI during the engine development and evaluation portion of the project. The following paragraphs describe the engine testing and the results.

2.5.1 Gasoline Engine Baseline/Verification Testing

The EVA-equipped engine was first tested in its gasoline configuration by Aura Systems. An increase in power and efficiency (approximately 10 percent) was found with the EVA engine operating over the lower speed portion of the operating range. Details of the engine testing conducted by Aura Systems are contained in Appendix A.

Upon receipt of the EVA engine from Aura Systems, SwRI tested the engine in its "as received" form. The purpose of this test was to verify that the performance of the engine and associated electronic systems was similar to that experienced at Aura Systems. This testing consisted of operating the engine (unloaded) at several engine speeds and verifying that the electronic subsystems were functioning properly. Subsequently, the engine modifications described in Section 2.4 were performed.

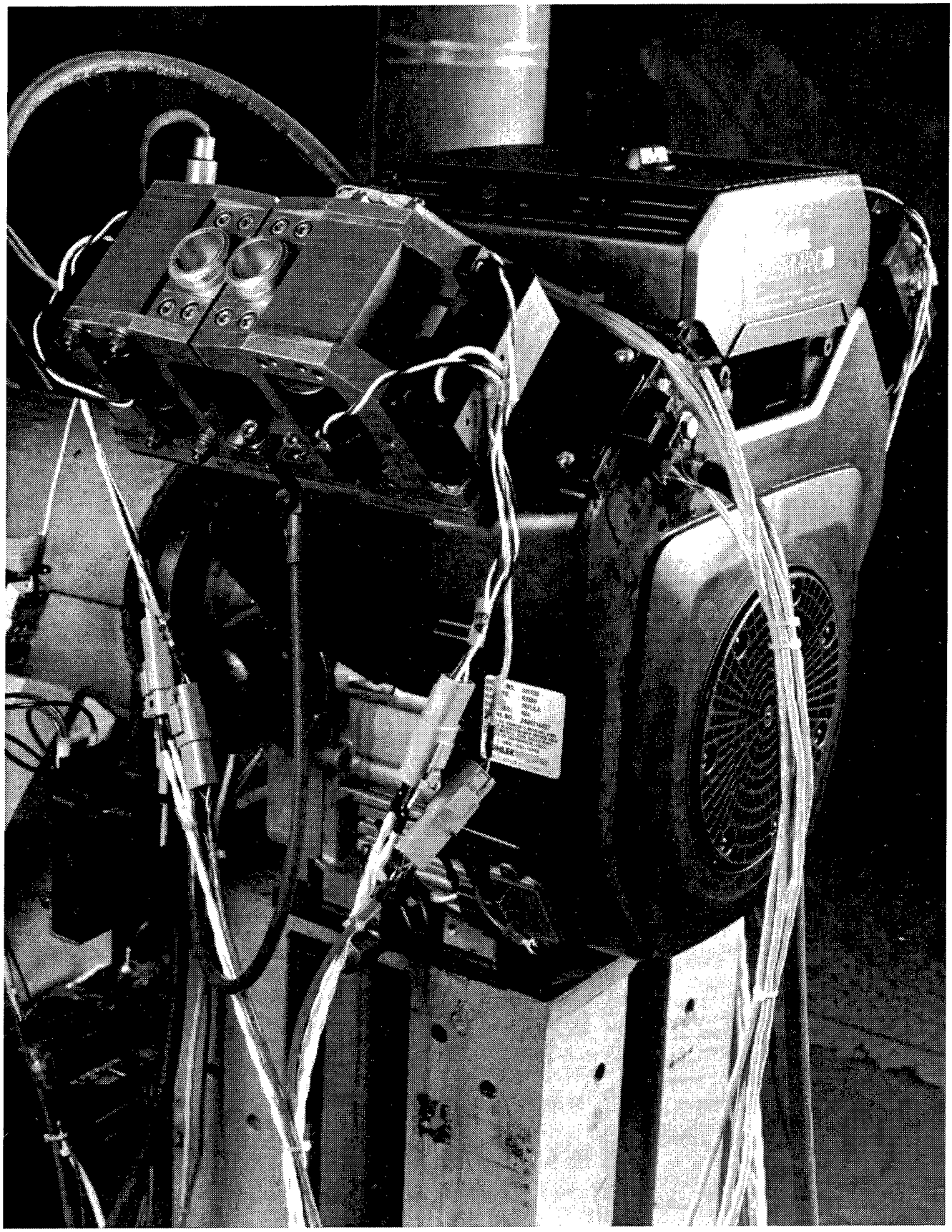

Figure 5. EVA Engine Installation

2.5.2 Natural Gas Engine Testing

Upon completion of the engine modifications, control-system installation, and engine checkout, the engine development and evaluation portion of the project was conducted. For this task, the natural gas configuration of the engine was tested.

The purpose of the engine testing was to investigate and quantify the benefits of the EVA-equipped engine versus the cam-driven engine. The focus of this work was to evaluate the engine power and efficiency increases that could be obtained with the EVA engine. This study did not focus on engine emissions since they are largely dictated by parameters such as catalyst conversion efficiency, fuel-air equivalence ratio, spark timing, compression ratio, and combustion chamber design. These parameters are not directly affected by the application of a VVT system. Furthermore, since such ultra-low (near zero) emissions levels were demonstrated with the Kohler CNG engine during the APU development project, emissions control was not felt to be an area in need of further exploration at that time.

Given the ability to independently control the valve events for the engine, strategies that had the potential to increase the power and efficiency of the engine were identified. The strategies were selected to improve either full load or part load (or both) performance. Three primary strategies were selected for investigation on the EVA engine.

The first strategy involved optimizing the valve events as a function of engine speed. This strategy showed any potential benefits associated with a "variable geometry cam," which would allow valve duration and timing to be tuned as a function of engine speed. This strategy involved no other changes to the operating strategy of the engine, i.e. the engine remained throttled. The first strategy will be referred to as optimized throttled operation, or the baseline strategy.

The second strategy involved operating the engine unthrottled at all conditions, and modulating load through early intake valve closing. At full load, the strategy was identical to the first strategy. However, as load was decreased, rather than closing the throttle to achieve a reduction

in mass flow through the engine, the duration of the intake event was shortened. The second strategy will be referred to as unthrottled operation using early intake valve closing (EIVC).

The third strategy involved operating the engine unthrottled, as in the second strategy. However, load modulation was accomplished via late intake valve closing. Similarly, at full load, the third strategy was identical to the first and second strategies. The third strategy will be referred to as unthrottled operation using late intake valve closing (LIVC). The following paragraphs discuss the strategies in detail.

2.5.2.1 Optimized Throttled Operation

Optimized throttled operation was the first strategy investigated on the EVA engine. The strategy involved manipulating the valve open and close angles for the intake and exhaust valves in order to achieve maximum full load torque at each engine speed.

Once the valve event map was calibrated, the volumetric efficiency map for the engine control system was calibrated. The volumetric efficiency map was used in a speed density calculation within the engine-control system's fueling algorithm. More specifically, the volumetric efficiency was used to compute the charge mass flow through the engine, thus affecting fueling.

Subsequently, the spark-timing map for the engine was calibrated. For each of the strategies tested, the spark timing was calibrated to be at MBT unless knock was experienced. In this case, the spark timing was set to knock limited timing for that condition.

Figure 6 shows the final intake valve open/close angle calibration map for the optimized throttled operation strategy. The independent variables for this map were engine speed and intake manifold pressure (in % bar). For each set of independent variable values, the valve open angle is displayed above the valve close angle. The angle convention used for the intake valve map was 0 degrees corresponding to TDC at the beginning of the intake stroke. A value of 180 degrees corresponds to BDC of the intake stroke. It should be noted that the values in this table correspond to the actual angle at which the EVA system achieved roughly 90 percent of the

KOHLER EVA CONTROLLER - INTAKE VALVE EVENT MAP

Engine Speed (RPM)

	800	1200	1600	2000	2200	2400	2600	2800	3200	3600	3800	4000
0.0	19	22	29	36	38	40	41	43	50	59	64	69
	202	179	178	180	182	184	186	189	197	202	205	208
20.0	19	22	29	36	38	40	41	43	50	59	64	69
	202	179	178	180	182	184	186	189	197	202	205	208
40.0	19	22	29	36	38	40	41	43	50	59	64	69
	202	179	178	180	182	184	186	189	197	202	205	208
60.0	19	22	29	36	38	40	41	43	50	59	64	69
	202	179	178	180	182	184	186	189	197	202	205	208
70.0	19	22	29	36	38	40	41	43	50	59	64	69
	202	179	178	180	182	184	186	189	197	202	205	208
80.0	19	22	29	36	38	40	41	43	50	59	64	69
	202	179	178	180	182	184	186	189	197	202	205	208
90.0	19	22	29	36	38	40	41	43	50	59	64	69
	202	179	178	180	182	184	186	189	197	202	205	208
100.0	19	22	29	36	38	40	41	43	50	59	64	69
	202	179	178	180	182	184	186	189	197	202	205	208

INTAKE VALVE %

Speed	0 rpm	Int_Open	19.0 CAD	MAP	1.6 psia
MAPBar	11.0 %Bar	Int_Cls	202.0 CAD	RunMode	STOPPED
EGO	0.205 volts	ThrotCmd	0.1 Volts	RunTime	00:00:00

Figure 6. Optimized Throttled Intake Valve Event Map

commanded position and not the angle at which the command signal to the servo controller was transitioned to the open or closed state.

In order to calculate the angle value at which the command signal to the servo controller was transitioned, the time response of the EVA system must be accounted for. Although the response time of the valve open-to-close transition was not identical to that of the valve close-to-open transition, and the response of the intake valves was not identical to that of the exhaust valves, the response times of the transitions were close enough to be treated as a constant. Actual differences in transition times were within roughly 10 percent. A first order approximation of an EVA valve's response to a command signal is approximately a 1-msec delay in series with a first order low pass filter having a time constant of approximately 1.2 msec. A time history of this response is shown in Figure 7. Therefore, in order to achieve 90 percent of the commanded position, the EVA system responds within roughly 4 msec of the commanded transition. This can be converted to crank angle degrees via Equation 1.

(1) EVA Transition Response in CAD = Rev/Min * Min/60000mSec * 360 CAD/Rev * 4 mSec

Therefore, at 1600 RPM, the command signal open and close transition angles could be computed by subtracting about 38.4 degrees from the table values. Similarly, at 3600 RPM a

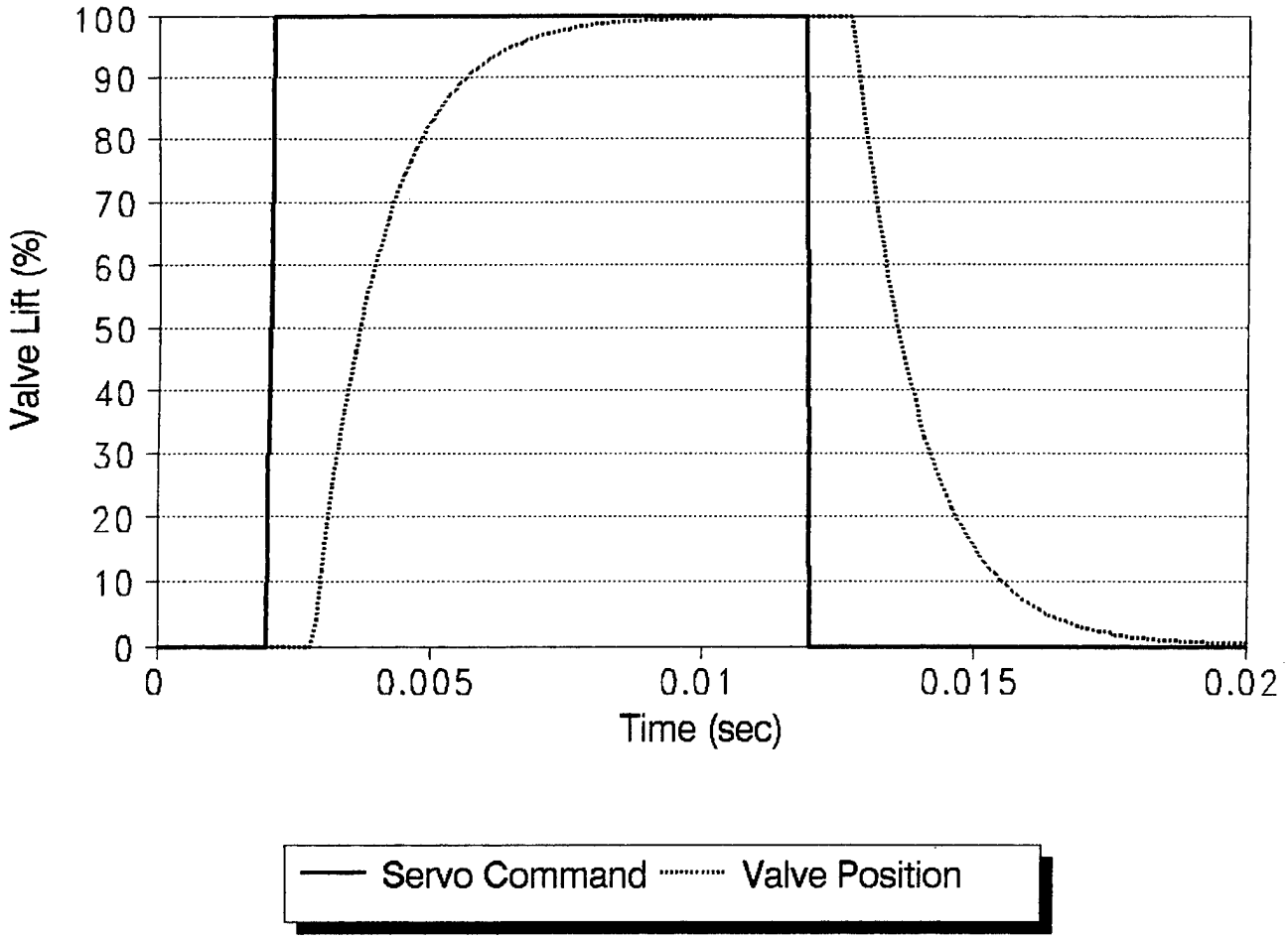

Figure 7. Simulated EVA Valve Response

value of 86.4 degrees must be subtracted from the table values. This compensation was done automatically by the SwRI engine/valve control system.

The final exhaust valve open/close angle calibration map is shown in Figure 8. The angle convention used for this data assumes that a value of 540 degrees corresponds to BDC of the exhaust stroke. A value of 720 degrees corresponds to TDC of the exhaust stroke. Valve close angles after TDC of the exhaust/intake stroke are represented by values greater than 720 degrees. Equation 1 can be used to calculate the angle values at which the command signal to the servo controller is transitioned.

In general, this strategy proved to be superior to the cam-driven natural gas engine at speeds up to approximately 2600 RPM. Above this speed, the EVA system's valve transition time response was actually slower than the cam-driven valves. This trend had a negative effect on

KOHLER EVA CONTROLLER - EXHAUST VALVE EVENT MAP

Engine Speed (RPM)

	800	1200	1600	2000	2200	2400	2600	2800	3200	3600	3800	4000
I 0.0	549	549	548	548	549	550	550	551	557	563	565	570
N	709	717	723	723	728	728	727	724	727	731	731	731
D 20.0	549	549	548	548	549	550	550	551	557	563	565	570
	709	717	723	723	728	728	727	724	727	731	731	731
V 40.0	549	549	548	548	549	550	550	551	557	563	565	570
A	709	717	723	723	728	728	727	724	727	731	731	731
R 60.0	549	549	548	548	549	550	550	551	557	563	565	570
	709	717	723	723	728	728	727	724	727	731	731	731
% 70.0	549	549	548	548	549	550	550	551	557	563	565	570
	709	717	723	723	728	728	727	724	727	731	731	731
80.0	549	549	548	548	549	550	550	551	557	563	565	570
	709	717	723	723	728	728	727	724	727	731	731	731
90.0	549	549	548	548	549	550	550	551	557	563	565	570
	709	717	723	723	728	728	727	724	727	731	731	731
100.0	549	549	548	548	549	550	550	551	557	563	565	570
	709	717	723	723	728	728	727	724	727	731	731	731

Speed	0 rpm	Exh_Open	549.0	CAD	MAP	1.6 psia
MAPBar	11.0 % Bar	Exh_Cls	709.0	CAD	RunMode	STOPPED
EGO	0.200 Volts	ThrotCmd	0.1	Volts	RunTime	00:00:00

Figure 8. Optimized Throttled Exhaust Valve Event Map

engine volumetric efficiency and reduced engine power output and thermal efficiency. Performance data on this strategy is contained in the Performance Comparison subsection of this report (section 2.5.2.4).

2.5.2.2 Optimized Unthrottled Operation using Early Intake Valve Closing (EIVC)

The second strategy involved operating the engine at wide open throttle at all conditions, and shortening the intake valve duration in order to reduce engine load. Since throttling is a primary efficiency reduction factor in a spark ignition engine (as compared to a diesel engine) an alternative to throttling, i.e. early intake valve closing, was investigated.

With the EIVC strategy, the valve close angle for the intake valves was changed as a function of engine speed and operator demand (or pedal position). The intake valve open angles, as well as the exhaust valve open and close angles were identical to those used in the optimized throttled strategy. The final intake valve open/close angle calibration map for the EIVC strategy is shown in Figure 9. Note the angle conventions used are the same as those described in section 2.5.2.1. As illustrated in the figure, at light load conditions, the commanded intake valve durations (intake close angle minus intake open angle) were quite small. In fact, this became a limiting factor, especially at higher engine speeds. Again, the physical limitation was the valve transition

KOHLER EVA CONTROLLER - INTAKE VALVE EVENT MAP

Engine Speed (RPM)

	800	1200	1600	2000	2200	2400	2600	2800	3200	3600	3800	4000
0.0	19	22	29	36	38	40	41	43	50	59	64	69
	24	27	43	53	58	63	67	72	82	91	96	101
20.0	19	22	29	36	38	40	41	43	50	59	64	69
	39	32	48	58	63	68	72	77	87	96	101	106
40.0	19	22	29	36	38	40	41	43	50	59	64	69
	63	66	85	92	93	98	94	91	99	118	113	118
60.0	19	22	29	36	38	40	41	43	50	59	64	69
	75	78	98	105	111	116	118	123	133	130	135	140
70.0	19	22	29	36	38	40	41	43	50	59	64	69
	84	87	110	113	114	130	123	128	138	143	148	153
80.0	19	22	29	36	38	40	41	43	50	59	64	69
	93	96	122	121	127	132	133	135	147	151	156	161
90.0	19	22	29	36	38	40	41	43	50	59	64	69
	107	110	138	138	142	146	147	149	161	166	171	178
100.0	19	22	29	36	38	40	41	43	50	59	64	69
	183	172	178	180	182	184	186	189	197	202	205	208

Speed	0	rpm	Int_Open	19.0	CAD	MAP	1.6	psia
MAPBar	10.9	%Bar	Int_Cls	32.0	CAD	RunMode	STOPPED	
EGO	0.197	volts	ThrotCmd	0.1	Volts	RunTime	00:00:00	

Figure 9. EIVC Intake Valve Event Map

time response for the EVA system. This characteristic shows up as a limitation in the level of load modulation, which could be accomplished with the EIVC strategy at high engine speeds.

As with the first strategy, upon completion of the valve event calibration map for the EIVC strategy, the volumetric efficiency map, and subsequently the spark timing map, was recalibrated. Again, the volumetric efficiency map was adjusted to accurately compute the mass flow of air and fuel through the engine. The spark timing map was adjusted to operate the engine at MBT timing at all conditions.

The EIVC strategy was found to be the best strategy in terms of maximizing part load efficiency. As previously stated however, the minimum intake valve duration limitation prevented light load/high speed operating conditions from being achieved with this strategy. Performance data and further analysis of this strategy are contained in section 2.5.2.4 of this report.

2.5.2.3 Optimized Unthrottled Operation using Late Intake Valve Closing (LIVC)

The third strategy involved operating the engine at wide-open throttle at all conditions, just as in the EIVC strategy. However, rather than shortening the intake valve duration, the durations were

lengthened in order to reduce engine load. Again, the motivation for this approach was to provide an alternative to throttling.

With the LIVC strategy, the valve close angle for the intake valves was changed as a function of engine speed and operator demand (or pedal position). The intake valve open angles, as well as the exhaust valve open and close angles, were identical to those used in the other strategies. The final intake valve open/close angle calibration map for the LIVC strategy is shown in Figure 10. Note the angle conventions used are the same as those described in section 2.5.2.1. As shown in Figure 10, the intake valve duration values become quite large as load (or operator demand) was decreased. This strategy is much more conducive to the characteristics of the EVA system in terms of its time response. However, the LIVC strategy did not prove to be quite as effective at increasing the part load efficiency as the EIVC strategy (described in section 2.5.2.4).

As with the previous strategies, upon completion of the valve event calibration map for the LIVC strategy, the volumetric efficiency map, and subsequently the spark timing map, was recalibrated. Again, the volumetric efficiency map was adjusted to accurately compute the mass flow of air and fuel through the engine. The spark timing map was adjusted to operate the engine at MBT timing at all conditions.

KOHLER EVA CONTROLLER - INTAKE VALVE EVENT MAP

	Engine Speed (RPM)											
	800	1200	1600	2000	2200	2400	2600	2800	3200	3600	3800	4000
0.0	19	22	29	36	38	40	41	43	50	59	64	69
I	300	307	310	308	312	316	318	320	324	322	321	323
N 20.0	19	22	29	36	38	40	41	43	50	59	64	69
D	288	295	298	294	298	302	301	301	295	293	304	306
40.0	19	22	29	36	38	40	41	43	50	59	64	69
V	276	283	278	280	283	286	283	281	285	283	291	293
A 60.0	19	22	29	36	38	40	41	43	50	59	64	69
R	254	261	240	258	264	270	266	264	265	268	273	275
70.0	19	22	29	36	38	40	41	43	50	59	64	69
%	240	247	236	246	251	257	258	260	255	260	261	263
80.0	19	22	29	36	38	40	41	43	50	59	64	69
	224	231	228	223	229	234	239	244	235	250	249	251
90.0	19	22	29	36	38	40	41	43	50	59	64	69
	202	210	208	213	218	223	226	229	225	231	232	234
100.0	19	22	29	36	38	40	41	43	50	59	64	69
	202	179	178	180	182	184	186	189	197	202	205	208

Speed	0	rpm	Int_Open	19.0	CAD	MAP 1.6 psia
MAPBar	10.9	%Bar	Int_Cls	293.5	CAD	RunMode STOPPED
EGO	0.198	volts	ThrotCmd	0.1	Volts	RunTime 00:00:00

Figure 10. LIVC Intake Valve Event Map

The LIVC strategy was superior to the optimized throttled strategy in terms of maximizing part load efficiency. However, the LIVC strategy was inferior to the EIVC strategy at the similar conditions. Performance data and further analyses of this strategy are contained in section 2.5.2.4 of this report.

2.5.2.4 Performance Comparison

Engine data has been included to show the performance of the EVA system relative to the cam-driven natural gas engine from the APU development project. Also, data has been included to show the attributes of each of the three EVA strategies relative to one another. In order to explain why strategies performed differently relative to one another, high-speed cylinder pressure data was acquired and is presented for each strategy. Finally, electrical power consumption data of the EVA system is presented and compared for each strategy.

It should be noted that all brake thermal efficiency (BTE) data for the engine was computed to account for the electrical power consumption of the EVA system. The engine brake thermal efficiency calculation used is shown in Equation 2.

(2) BTE = BHP/(FuelFlow*QLHV/2545 + EVA Volts*EVA Amps/746)

where:

- BHP - Engine Brake Horsepower Output (hp)
- FuelFlow - Engine Fuel Flow (Lbm/Hr)
- QLHV - Fuel Lower Heating Value (roughly 20500 BTU/Lbm)
- EVA Volts - Average DC Voltage to the EVA Power Electronics (Volts)
- EVA Amps - Average DC Current to the EVA Power Electronics (Amps)

2.5.2.4.1 Full Load Performance Comparison

The full load performance of the EVA system was compared to the cam-driven natural gas engine in terms of torque, power and thermal efficiency. Since each of the three EVA strategies

were identical at full load, only one EVA strategy was included. The comparison data is shown in Figure 11. As demonstrated by the data, performance of the EVA engine is superior to the cam-driven engine up to roughly 2600 RPM. Above this speed, the EVA engine's performance is inferior to the cam-driven engine. As previously stated, this is due to the time response of the EVA system.

The stock Kohler cam profile was measured to quantify the valve 10-percent to 90-percent transition time. Based on these measurements, it was determined that the 10-percent to 90-percent valve transition and 90-percent to 10-percent transition occurred over roughly 60 crank angle degrees of travel. Since the time response of the cam-driven valves was a function of engine speed, the speed at which the valve transition times were equal (cam-driven valves versus EVA driven valves) could be calculated. Equation 3 can be used as an indication of this engine speed. It should be noted that Equation 3, though simple, should provide a good estimation of the engine speed at which the cam-driven valves would provide breathing advantages over the EVA system. To compute this engine speed exactly, the valve lift of each approach must be integrated and compared.

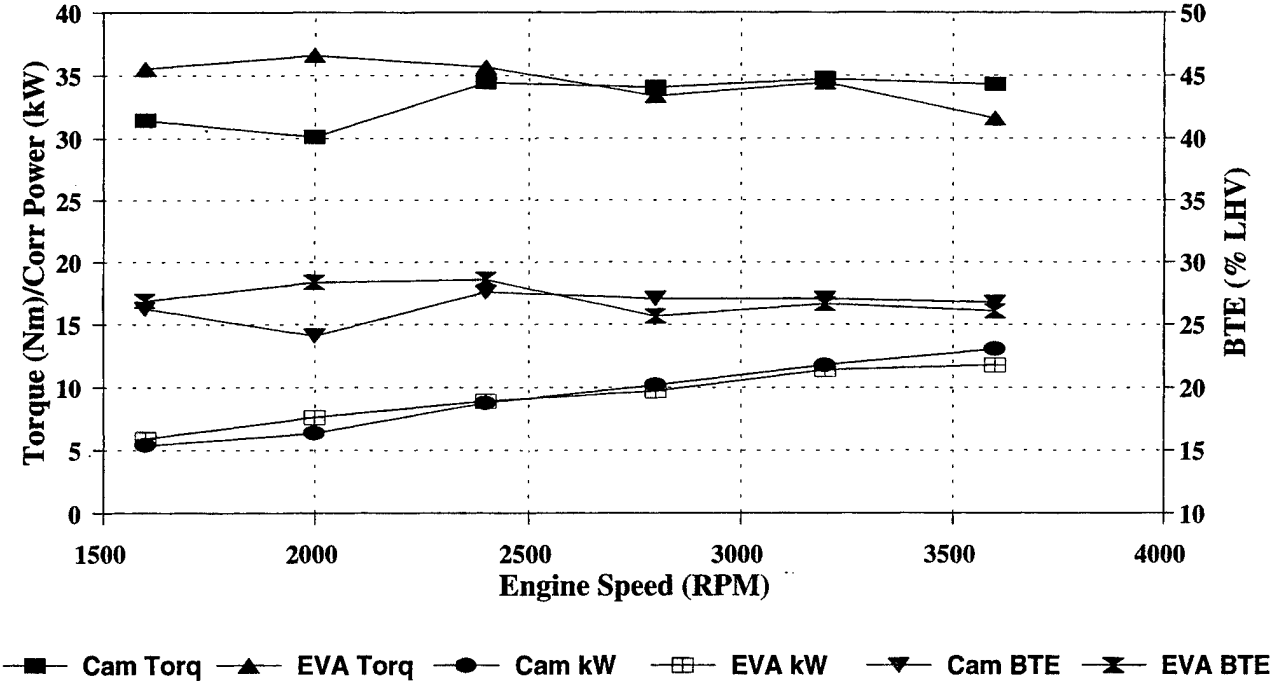

Figure 11. CH22 NG Full Load Comparison: CH22 Stock Cam vs CH22 EVA Engine

(3) Engine Speed = 60 CAD / (Min/60000mSec * 360 CAD/Rev * 4 mSec) = 2500 RPM

From Equation 3 it can be seen that, above engine speeds of approximately 2500 RPM, the EVA system valve response is slower than the cam-driven valves. This is consistent with the engine test results.

2.5.2.4.2 Part Load Performance Comparison

The part load efficiencies of the three EVA strategies were compared in order to show the relative performance of each strategy. Since all three strategies were identical at full load conditions, the performance data at full load should have been equivalent. However, due to typical factors such as ambient temperature, pressure, humidity and knock, as well as unusual factors such as engine aging and performance degradation over time, performance data fluctuations at full load were observed. Engine aging and wear are not typically factors in acquiring engine performance data. However, considering that the longest engine operational life of any of the Kohler engines tested during the EVA and APU development programs was less than 100 hours, the aging of the engine was not a negligible factor. Hence performance comparison data was re-run several times during the project to quantify the repeatability of the data and characteristic trends. The final performance data for each of the strategies were taken contiguously, with essentially no extraneous engine operation between the testing of each strategy. However, engine knock was experienced during the final testing of the optimized throttled strategy at full load. Therefore, the spark timing was retarded with the baseline strategy at the full load condition only. All other spark-timing values were set at MBT.

The part load performance comparison for the three EVA strategies is shown in Figure 12. The figure shows relative performance for engine speeds of 1600 rpm, 2400 rpm, and 3600 rpm respectively. The engine brake thermal efficiency (BTE) as a percentage of fuel lower heating value as a function of engine torque is shown for each strategy. Again, the electrical power consumed by the EVA power electronics was taken into account in the BTE calculation as shown in Equation 2. As expected, with the throttled (baseline) case, the efficiency values decrease as engine load is reduced. The exception to this is at full load, where spark timing was retarded from MBT in order to prevent knock. The spark timing adjustment is also evident in the

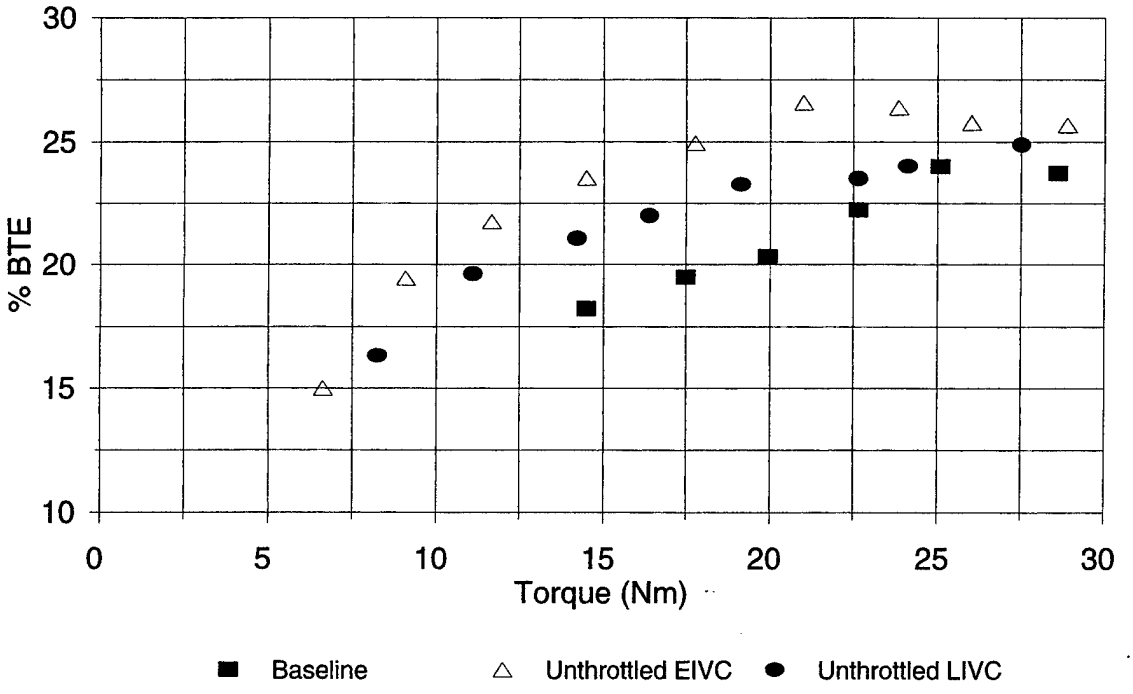

Figure 12a. CH22 NG Efficiency Comparison: Baseline vs EIVC vs LIVC (1600 RPM)

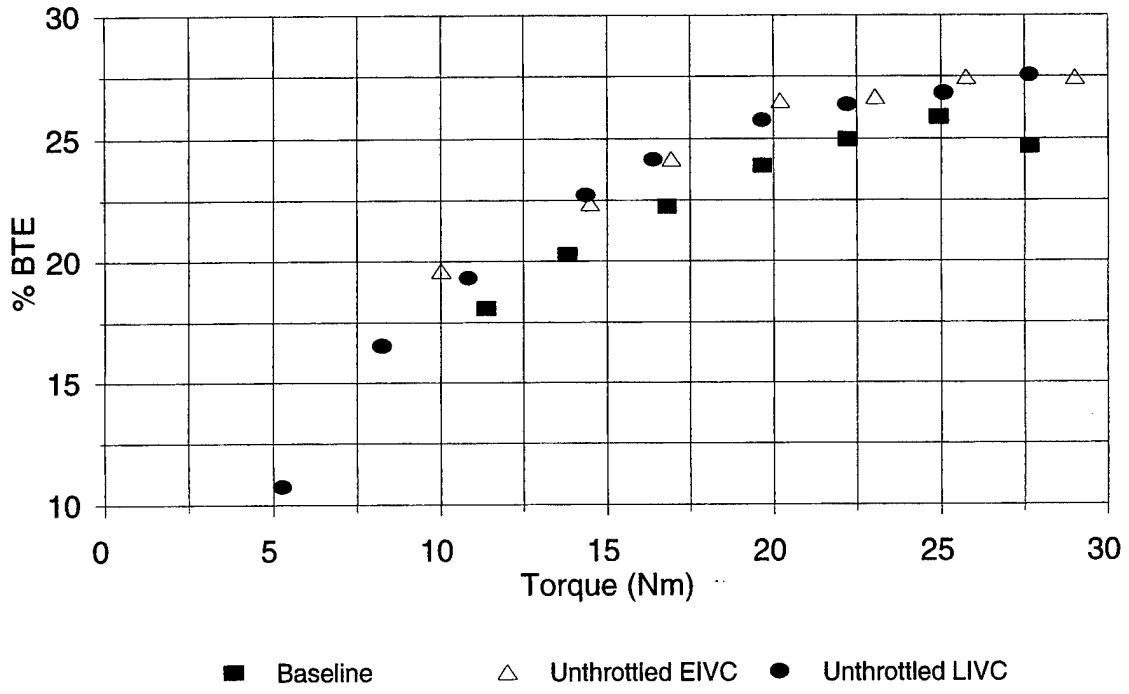

Figure 12b. CH22 NG Efficiency Comparison. Baseline vs EIVC vs LIVC (2400 RPM)

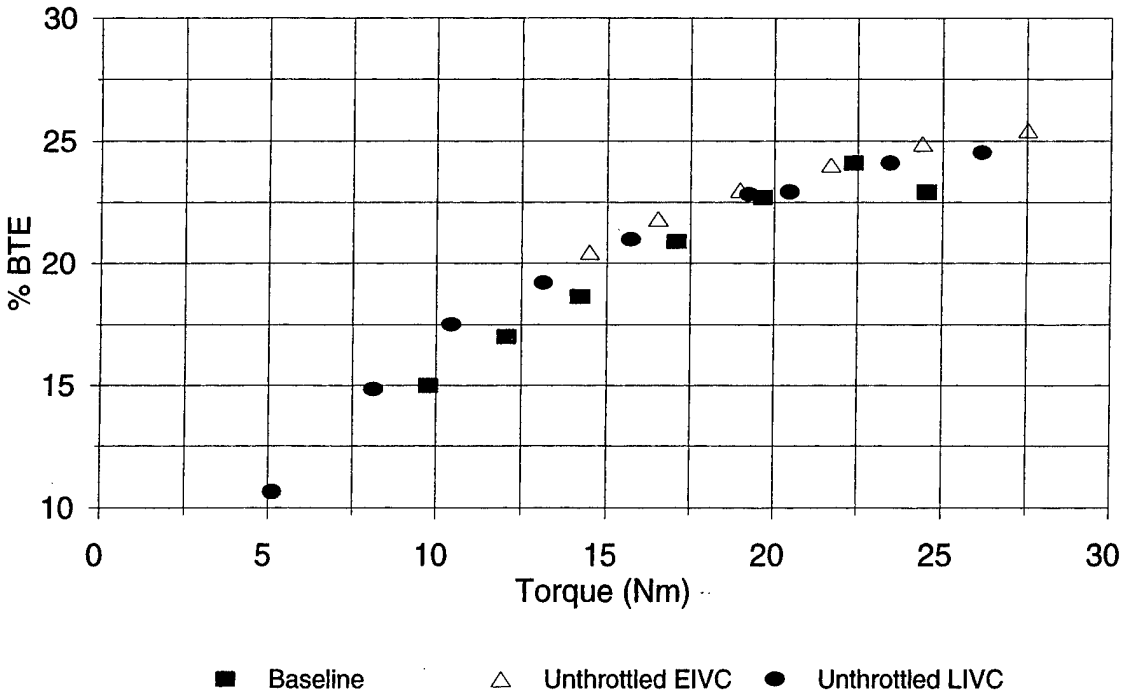

Figure 12c. CH22 NG Efficiency Comparison: Baseline vs EIVC vs LIVC (3600 RPM)

maximum torque values for the baseline strategy, i.e. they are slightly below the maximum torque values for the EIVC and LIVC strategies. The general trend is the same for the two unthrottled strategies. However, the maximum efficiency point was shown to be below maximum torque for the EIVC strategy at 1600 RPM. In addition, the efficiency reduction, as load was decreased, was found to be less with the unthrottled strategies. In fact, Figure 12a shows that the EIVC strategy represents a maximum improvement of roughly 20 percent over the 50-percent to 80-percent load range, as compared to the baseline strategy. This trend, seen in Figure 12b and 12c, is consistent as engine speed is increased, but the magnitude of the improvement is diminished. The LIVC strategy was also shown to be superior to the baseline strategy. The engine data shows that the LIVC strategy is comparable in performance to the EIVC strategy, but slightly less effective than the EIVC strategy at1600 rpm. The LIVC strategy, however, is more conducive to implementation with the EVA system. As shown in Figure 12b, at 3600 RPM, the EIVC strategy could only be used to achieve loads down to roughly 50 percent. At the 50-percent load point, the EVA system was incapable of reducing the duration of the intake valve event any further. However, with the LIVC strategy, the valve

events become longer as engine load is reduced. This can be easily achieved with the EVA system.

The magnitude of the part load efficiency improvements measured with the throttleless EVA strategies over the baseline strategy was larger than expected. With efficiency improvements as high as 20 percent, this represents a significant improvement in the in-use fuel consumption of the engine. Given the test results, it was then necessary to gather more detailed in-cylinder data to provide further validation and explanation of the results obtained.

2.5.2.4.3 High Speed Data

Based on the results of the part load testing, the question of why the throttleless EVA strategies were significantly superior to the baseline remained. In order to answer this question, it was decided that high speed data would be taken on each strategy. High speed data, in the form of cylinder pressure versus crank angle, were recorded for each strategy over a specified set of operating conditions. In order to acquire this data, a Kistler model 6051 pressure transducer was built into the spark plug for cylinder #1 of the engine. In addition, an optical encoder was coupled to the engine crank shaft.

At a fixed load or BMEP level, in order to provide superior efficiency, the throttleless EVA strategies would have to provide either a decrease in pumping work, a decrease in friction, or both, as compared to the optimized throttled (baseline) strategy. A decrease in maximum cylinder pressure, for a given load condition, would yield a reduction in friction as well as reduced dissociation within the cylinder. Both of these effects would result in increased thermal efficiency.

As an initial look at the relative performance of the EVA strategies using the high speed data, log P/log V (or P-V) diagrams were generated for each operating condition. P-V diagrams show the cylinder pressure versus the cylinder volume over the entire engine cycle. Visual inspection of the plots indicated that the area of the pumping loop was lower for the throttleless strategies. In addition, peak cylinder pressure values were significantly lower for the throttleless strategies. Figure 13 shows P-V diagrams for the baseline, EIVC, and LIVC strategies respectively. The

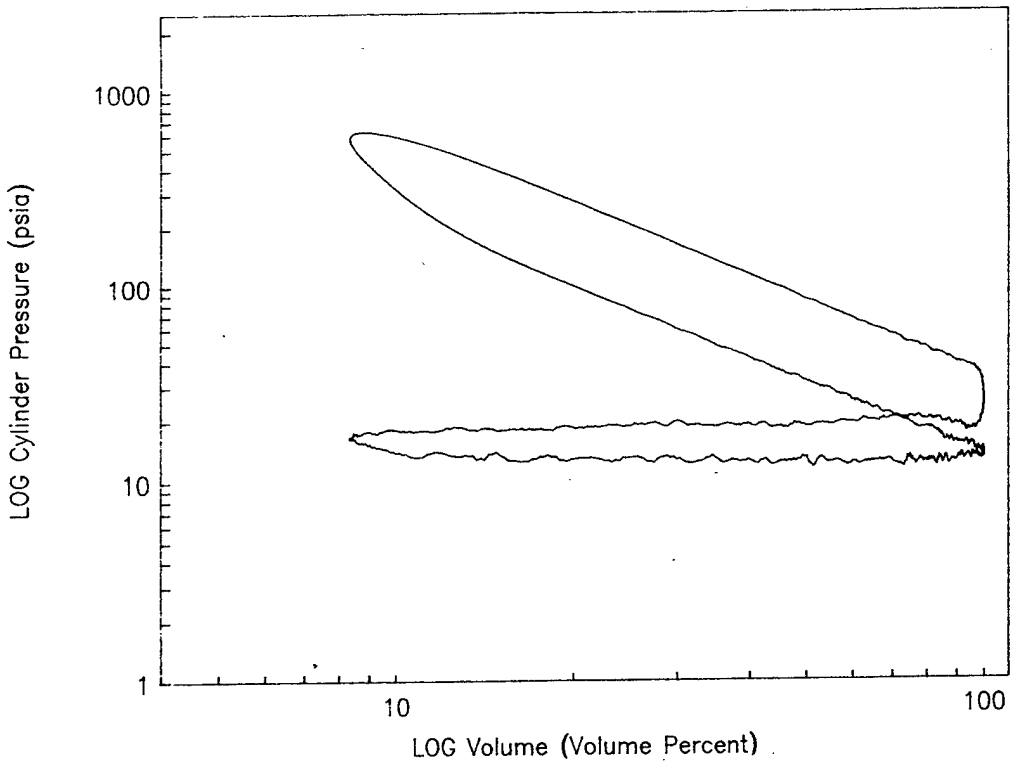

Figure 13a. Pressure/Volume Diagram: Baseline Strategy

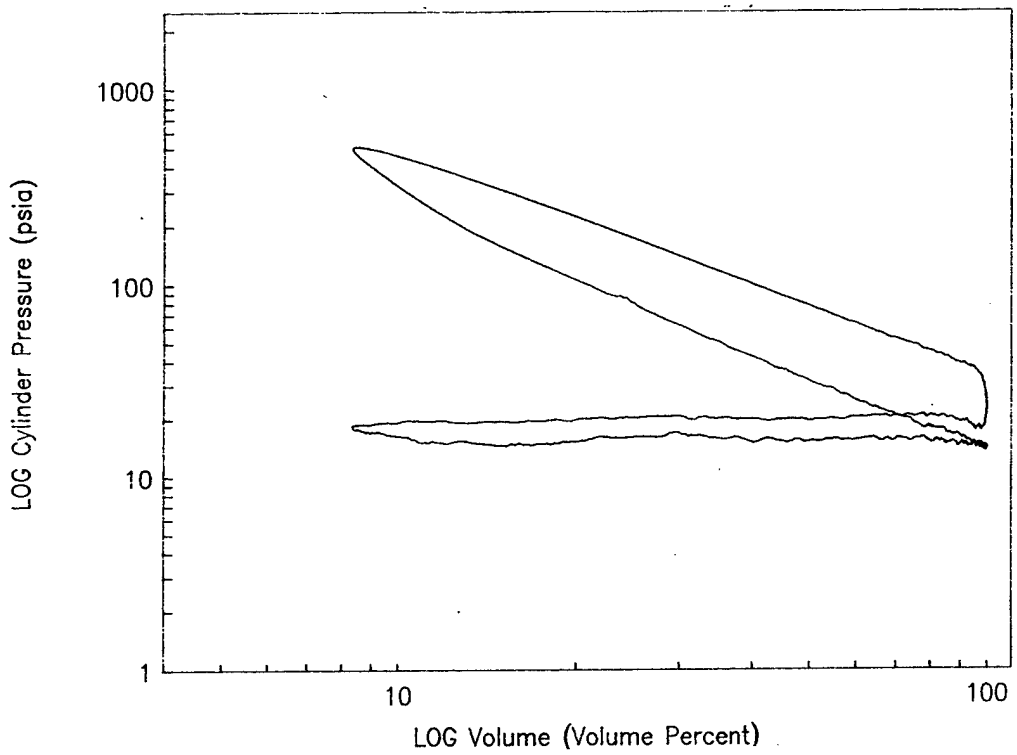

Figure 13b. Pressure/Volume Diagram: EIVC Strategy

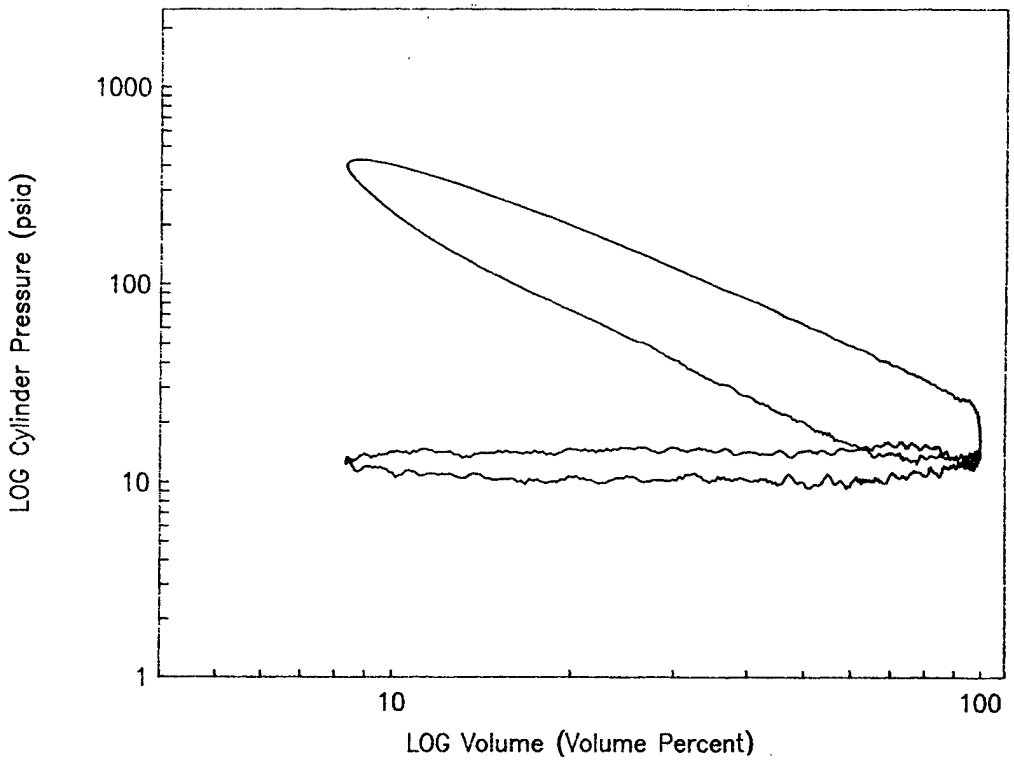

Figure 13c. Pressure/Volume Diagram: LIVC Strategy

engine operating condition was 2400 RPM/60-percent load. This condition was chosen to show the significant differences in the strategies. A detailed analysis of the high speed data verified the initial hypothesis formulated from analysis of the P-V diagrams.

The results of the high speed data analysis revealed that the throttleless EVA strategies provided both a reduction in pumping work or pumping mean effective pressure (PMEP), as well as a significant reduction in maximum cylinder pressure for part load conditions, as compared to the optimized throttled (baseline) strategy. Table 1 contains pumping work data for each of the three EVA strategies at various load conditions. The data is presented for an engine speed of 2400 rpm. Note that the PMEP values are negative, indicating that work had to be done by the piston in order to complete the gas exchange through the engine.

Table 1. Pumping Mean Effective Pressure (psi) vs Load at 2400 rpm						
% Load / EVA strategy	50%	60%	70%	80%	90%	100%
Baseline	-7.70	-6.56	-5.88	-5.40	-5.12	-4.36
EIVC	-4.67	-4.53	-4.51	-3.75	-4.09	-4.35
LIVC	-3.39	-3.61	-3.76	-4.01	-2.90	-4.56

The data shows that at 100-percent load, the pumping work of each strategy is approximately equivalent. However, as load is reduced, the EIVC strategy shows as much as a 39-percent reduction in pumping work, as compared to the baseline case. Similarly, the LIVC strategy shows as much as a 56-percent reduction, as compared to the baseline.

In addition to the reduction of pumping losses, the throttleless EVA strategies also achieved given part load conditions, with significantly lower peak cylinder pressure values than the baseline. As previously stated, this is also a significant factor in achieving increased thermal efficiency. Table 2 shows the peak cylinder pressure values as a function of load for each of the three strategies at 2400 rpm. It should be noted that 2400 rpm was chosen since it is an intermediate speed for the engine. The same trends, in terms of PMEP, peak cylinder pressure, and efficiency were observed at all speeds tested.

Table 2. Peak Cylinder Pressure (psia) vs Load at 2400 rpm						
% Load / EVA strategy	50%	60%	70%	80%	90%	100%
Baseline	589.7	657.7	710.1	714.9	667.3	623.9
EIVC	480.0	506.8	551.3	599.1	625.8	662.9
LIVC	387.5	428.3	493.8	542.6	586.1	587.9

As shown in Table 2, significant reductions in peak cylinder pressure, as compared to the baseline, were observed for the throttleless EVA strategies. As previously stated, reduction in peak cylinder pressure has two effects.

- It reduces friction within the cylinder via reduction of force between the piston rings and cylinder liner. It also reduces bearing friction within the engine.

- Lower cylinder pressures are also indicative of lower in-cylinder gas temperatures; lower gas temperatures reduce the amount of heat transfer and molecular dissociation during the cycle. Both heat transfer and dissociation reduce the amount of useful energy available to be extracted as work by the piston. The combination of these two factors yields significant changes to engine thermal efficiency.

From the analysis of the high-speed engine data, it is apparent that the throttleless EVA strategies had significant advantages over the baseline strategy in terms of reduced pumping work and reduced peak cylinder pressure. These differences adequately explain the thermal efficiency advantages observed using the EIVC and LIVC strategies.

2.5.2.4.4 EVA Power Consumption

One of the most important attributes of any VVT system is the power consumption of the system. In order to quantify performance improvements made from using VVT, the power consumed by the VVT system must be considered. As discussed in section 2.5.2.4, the efficiency data presented in this report took into account the average electrical power consumed by the EVA power electronics and electromagnets. For clarity, the actual EVA power consumption data is presented in this section of the report.

Through experimental testing, it was determined that the EVA power consumption was solely a function of engine speed. That is, for a given engine speed, the power consumption was essentially constant for all load conditions. As expected, the power consumption increased linearly with increasing engine speed. The actual EVA system power consumption, as a function of engine speed, is illustrated in Figure 14. As shown in the figure, the power consumption for each of the three EVA strategies is roughly equivalent.

Although the power necessary to actuate the cam-driven valve train for the Kohler engine was not measured, Aura Systems' data indicates that a standard automotive 16-valve engine operating at 2500 RPM consumes roughly 3 kW. Assuming that the power consumption scales down linearly as a function of the number of valves, roughly 0.75 kW

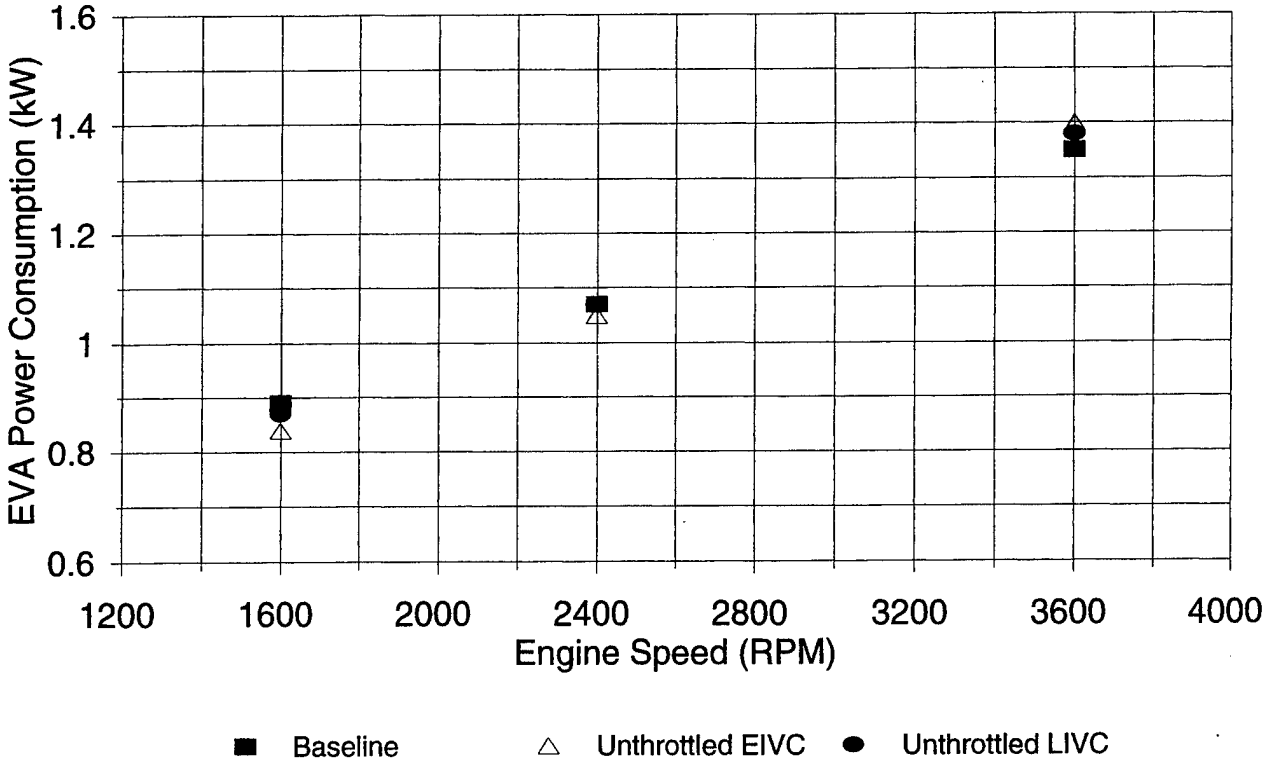

Figure 14. EVA Electrical Power Consumption: Baseline vs EIVC vs LIVC

would be consumed by a 4-valve engine. This compares to roughly 1.1 kW from the data in Figure 14. From this first order comparison it appears that the power consumption of the EVA system is quite high. This was confirmed by Aura Systems, and potential power consumption improvements are discussed in Appendix A.

3.0 SUMMARY

A prototype EVA system was applied to a Kohler engine by Aura Systems. The engine was converted to operate on natural gas and tested in the laboratory environment at Southwest Research Institute.

A prototype engine/valve control system was developed by SwRI for control of engine fueling, ignition, throttle, and valve event functions. The prototype controller was designed around a personal computer platform for maximum flexibility in control

algorithm development, control system calibration, and sensor and actuator flexibility. The engine/valve controller was designed to interface directly with the EVA servo controller.

The performance of the EVA engine was compared to a stock Kohler gasoline engine, as well as a modified Kohler natural gas engine. EVA engine performance was found to be superior to the cam-driven engine at low engine speeds and inferior at high engine speeds. The reason for this is related to the response time of the EVA valves.

Three EVA strategies were evaluated to increase part load engine performance. Two of the strategies involved unthrottled operation in conjunction with Miller Cycle operation. The EIVC strategy produced the best results in terms of part load efficiency improvements. However, the EIVC strategy could not achieve the full operational range of the engine.

4.0 RECOMMENDATIONS

The EVA system was successfully demonstrated on the Kohler engine. Performance improvements were quantified with the system, over a similar engine with a cam-driven valve train. However, further possible applications and potential strategies for the EVA system are included in the succeeding paragraphs.

First, an alternative engine should be considered. Because of the short operating life of the Kohler engine, caused by the high duty cycle test environment of the evaluation program, performance variability and overall life of the engine became significant factors. In fact, during the evaluation program, it was necessary to replace the Kohler engine and transfer the EVA hardware to a new engine. This meant that a large amount of performance data had to be re-run. Besides the durability of the engine, since the EVA engine performance was better at low engine speeds, a lower-speed engine (possibly a heavy duty engine) may be a better candidate.

Some other potential strategies that could be evaluated using the EVA system are skip fire, residual fraction control, and true Miller Cycle operation. Using the EVA system for skip fire would allow a cylinder or set of cylinders to be de-activated as desired. Therefore, when using skip fire, the effective load of the operational cylinders is increased for a given engine load. Various forms of this technique have been successfully implemented. The most common form simply involves the removal of fueling from the skip fire cylinder(s). This technique has been proven to be effective at increasing part load efficiency. The shortcoming of this simplified approach is that the skip fire cylinders still consume power due to air exchange and actuation of the valve train. With the EVA system these losses could be eliminated, and the full benefits of skip fire could be realized.

The second potential strategy that could be investigated with the EVA system is residual fraction control (similar to exhaust gas recirculation [EGR] control). The emissions benefits of EGR are well documented, but the method for achieving and controlling the desired EGR rates create problems on the engine and force the engine development engineer to sacrifice efficiency and performance. With the EVA system, since the exhaust valve events can be varied, the residual gases (or EGR) trapped within the cylinder could be controlled directly. This would eliminate the need for designing a high or low pressure EGR loop to introduce the exhaust back into the engine intake. This technique would likely represent the best approach for transient and true "cycle-by-cycle" control of residual fraction (or EGR).

The third potential strategy that the EVA system lends itself to is in full Miller Cycle operation. Although "Miller Cycle type" operation was investigated in this project, the emphasis was on applying this technique to eliminate the need for throttling. With true Miller Cycle operation, however, significant increases in geometric compression ratio (hence expansion ratio) are made to increase efficiency.

APPENDIX A
AURA SYSTEMS' FINAL REPORT

AURA
SYSTEMS INC.
2335 Alaska Avenue, El Segundo CA 90245

Design and Performance of a Kohler C22 Engine

Retrofitted With an Electromagnetic Valve Actuation System

Presented to

South West Research Institute
San Antonio, Texas 78228-0510
USA

October 1996

AURA
SYSTEMS INC.
2335 Alaska Avenue, El Segundo CA 90245

Approaches to Improved Configuration of an Electromagnetic Valve Actuation System prepared for South West Research Institution

Table of Contents

AURA
SYSTEMS INC.
2335 Alaska Avenue, El Segundo CA 90245

1.0 Summary

The Kohler C22 two cylinder, two valve per cylinder, four stroke engine, with a rated peak power of 16.8 horse power at 4,000 RPM was the engine selected for this project. This engine was retrofitted by Aura Systems with a turnkey Electromagnetic Valve Actuation system to demonstrate variable valve timing and to demonstrate the potential for improved engine performance for South West Research Institute.

Dynamometer testing of the non-optimized EVA equipped Kohler engine was compared with baseline data from a stock Kohler engine. The EVA equipped engine provided up to 15% more horsepower and torque and up to 30% reduction in pre-catalytic converter emissions (HC, CO and NO_x).

The purpose of this paper is to describe Aura System's development of an Electromagnetic Valve Actuation (EVA) system for the Kohler C22 engine, and to provide a suggested road map for improvement. As the report details, the following improvements to the EVA design are expected in future efforts:

- Electrical Power consumption could be reduced up to 40%.
- Actuator size and weight could be reduced up to 50%.

2.0 Basic Operating Principle of EVA.

The basic components of the electric valve actuator are two electromagnets, an open spring, a close spring, an armature, an armature guidance system, a valve, and a valve guidance system. The armature resides between the two electromagnet pole faces, such that energizing either electromagnet will pull the armature in the direction of the energized electromagnet. Note that electromagnets can only attract the armature, repulsion is not possible. The armature guidance system allows for motion of the armature between the two electromagnets such that the surface of the armature is parallel to the surface of the electromagnets when the surfaces make contact.

The force of attraction (F_{em}) between an electromagnet and an armature is inversely proportional to the square of the distance between them (r):

$$F_{em} \propto \frac{1}{r^2}$$

Because the electromagnet force decreases with distance from the armature, the electromagnet is best suited for applying force when the armature is close to the electromagnet. An electromagnet which, by itself, could force open an exhaust valve would be far too large to be practical. Therefore, springs are used to push the armature away from the electromagnet. As can be seen from Figure 1, drawings showing a simple EVA configuration in the open, closed, and neutral positions, the springs are arranged to keep the armature centered between the electromagnets. When the open electromagnet is energized, the armature is pulled toward the open electromagnet (Figure 1, left). To close the valve, the open electromagnet is de-energized and the lower (close)

spring pushes the armature towards the closed electromagnet. Without energizing the close electromagnet, the armature will begin to oscillate in simple harmonic motion at a frequency determined by $$f = \frac{1}{2\pi}\sqrt{k/m}.$$

where k is the combined spring constant of the upper and lower springs, and m is the total moving mass comprised primarily of the armature, approximately half the combined spring mass, and the valve. The transition time for the valve to open or close is approximately determined by $$t = \pi\sqrt{m/k} = \frac{1}{2f}$$

assuming that damping is negligible, or is countered by the applied electromagnet force. To "catch" the armature, the close electromagnet is energized to provide enough force to replace energy lost due to friction. By precisely controlling the amount of energy applied to the armature, the armature landing velocity (equal to the valve seating velocity) can approach zero.

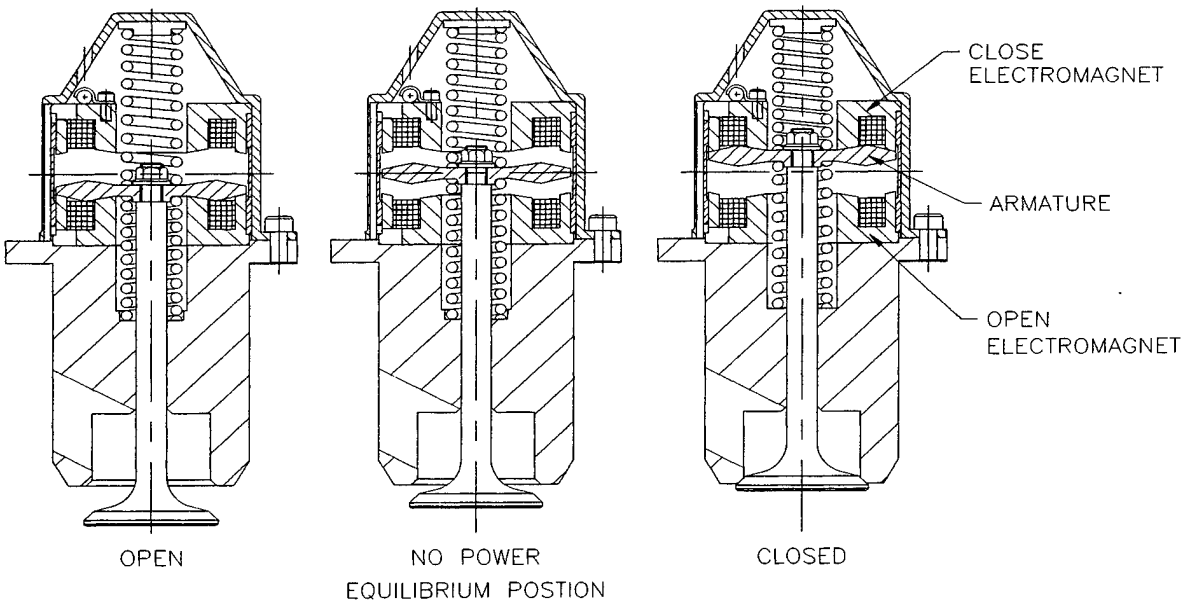

Figure 1. Basic EVA concept.

The static force requirement for the electromagnets can easily be determined from a free body diagram. The result is approximately

$$F_{em} = F_{springs} = k_{total}\frac{lift}{2}, \quad where$$

$$k_{total} = k_{top} + k_{bottom}$$

Electromagnetic force is proportional to electromagnet pole face area, so from the above expressions, several observations can be made.

- To decrease transition time either stiffer springs or a lighter mass are required.
- To increase lift and keep transition time constant requires a larger electromagnet force, which in turn requires a larger and heavier armature, which subsequently requires heavier and stiffer springs.
- Moving mass should be kept to a minimum.

The above equations may not hold true for valves operating against large residual exhaust pressures. The deviation will depend on the magnitude of required opening force.

2.1 EVA Electronics Overview

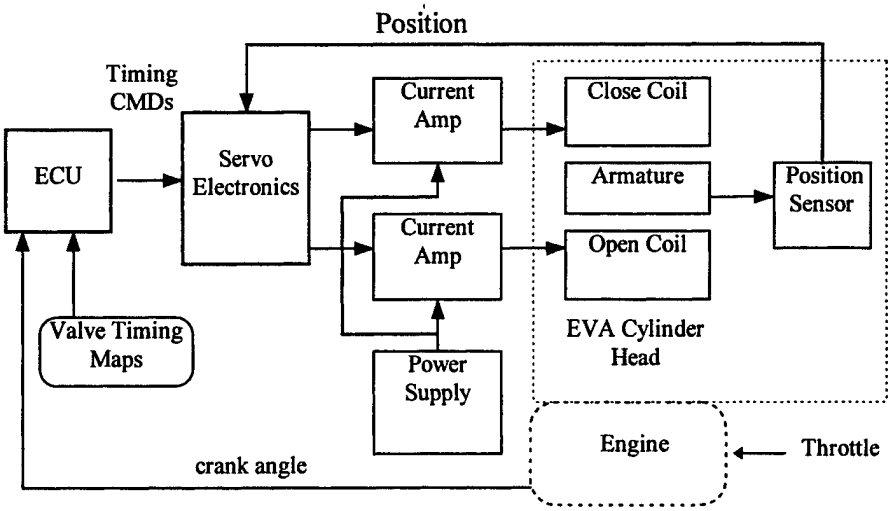

Figure 2. EVA Electronics Configuration.

Figure 2 illustrates the basic EVA electronics configuration. The Electronic Control Unit (ECU) generates valve timing commands corresponding to crank angles defined in two dimensional tables called maps. Figure 3 is an example of a valve timing map for intake open angle. Armature positions are monitored by a eddy current sensor, these position signals are fed to the

servo electronics box, along with the ECU commands. The servo electronics process this information and generate the appropriate actuator coil current commands for the current-amplifiers which drive the electromagnet coils.

Engine RPM Columns

	100	600	800	1000	1200	1400	1600	1800	2000	2200
Manifold Absolute Pressure										
100 KPa	320°	320°	319°	319°	316°	319°	315°	310°	310°	309°
130 KPa	320°	320°	319°	319°	316°	319°	315°	310°	310°	309°
160 KPa	320°	320°	319°	319°	316°	319°	315°	310°	310°	309°
190 KPa	320°	320°	319°	319°	316°	319°	315°	310°	310°	309°

Figure 3. Intake Valve: Fully Open Angle versus manifold pressure(rows) and RPM (columns). Angles are measured in Degrees Before TDC on the Compression Stroke

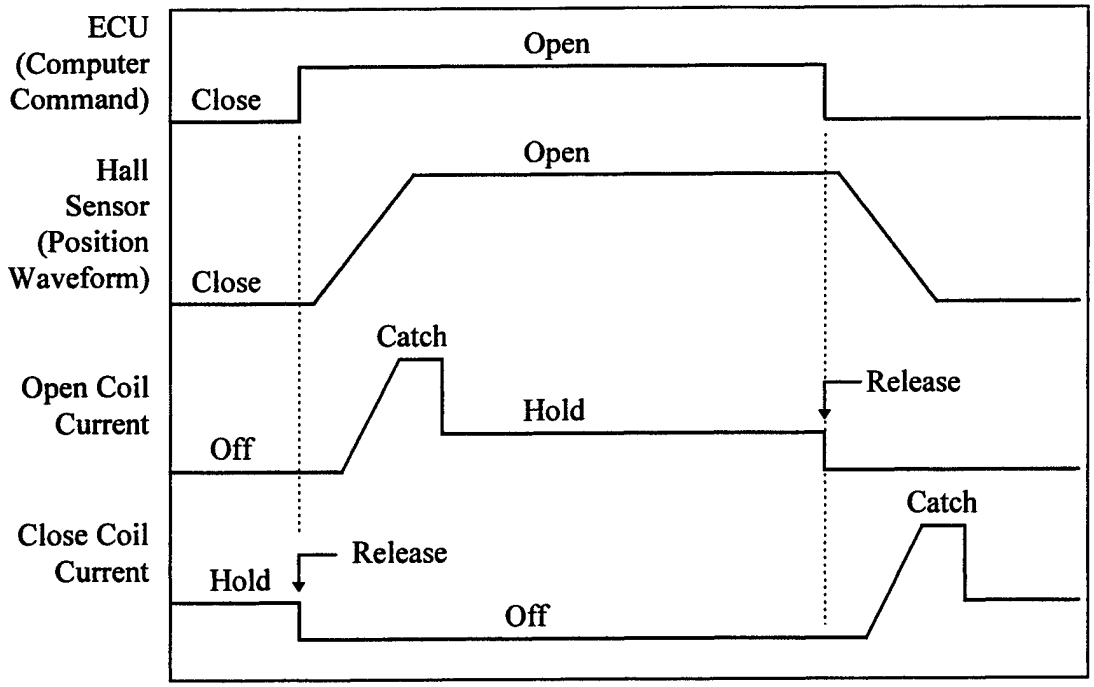

Figure 4. EVA Example Wave forms - Position and Current vs. Time

Figure 4 illustrates typical EVA operating wave forms. Upon receiving the valve "Open" command from the ECU, the "Close" electromagnet current is discharged to "Release" the armature so that the spring can push it toward the "Open" position. A high pulsed current is applied to the "Open" coil to "Catch" the armature with minimum energy and impact. After the armature has landed, the coil current is reduced to a low "Hold" level to maintain the armature

position. When the ECU command changes state, a similar process is performed to close the valve.

3.0 Actuator Development

At the beginning of the program, a mechanical layout of a cylinder head using cylindrical electromagnets similar to those shown in figure 5 was completed. At this time, it was determined that the cylindrical actuators of adjacent valves would have to be offset in height, or stacked, (as shown in figure 5) in order to provide adequate electromagnetic force. The mechanical complexity of this design motivated a search for a better configuration.

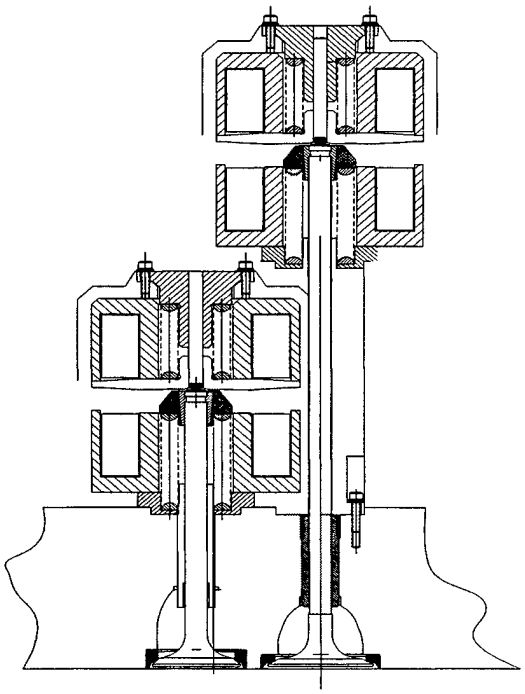

Figure 5. Initial Actuator Layout with Cylindrical Actuators

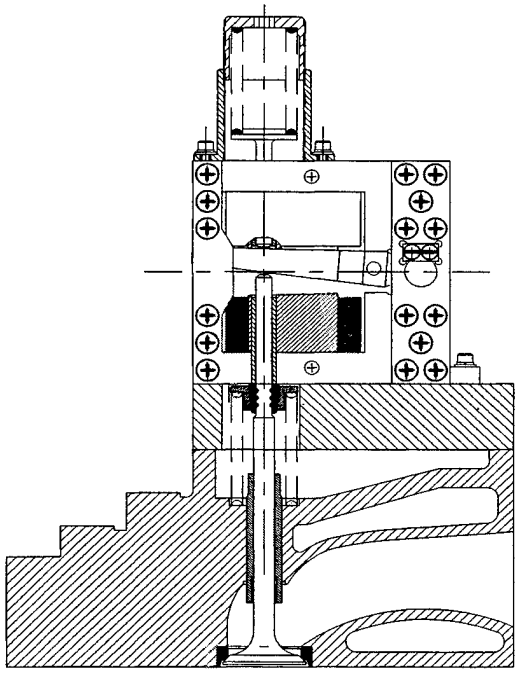

Figure 6. VIRAD Layout

The first new design approach used a rotating armature rather than a translating armature, and was given the acronym VIRAD, short for "Valve Inside Rotating Armature Design." A prototype of this design was built and tested, and is shown in figure 6. The prototype had several problems, the primary one being the magnetic force generated was insufficient to allow operation with the required springs. One negative packaging characteristic of this design was that the upper spring rested on top of the upper electromagnet, both adding height to the actuator assembly and requiring a push rod to connect the top spring to the armature. Finally, power

consumption of this design was very high due to eddy currents generated in the electromagnet's solid steel core. The VIRAD prototype was well suited for a Hall effect sensor, and the sensor operation was verified.

Since a redesign of the VIRAD prototype was necessary due to insufficient electromagnetic force, a solution which improved packaging and was suitable for laminated construction was sought. The fruit of this labor, shown in figure 7, was a design which shifted the springs from above and below the electromagnets to directly adjacent to the electromagnets. This design, which was used on the prototype engine, was given the acronym VORAD, short for "Valve Outside Rotating Armature Design." Though a larger actuator than the VIRAD prototype, power consumption was markedly reduced. The Hall effect position sensor output was more distorted by coil current than in the VIRAD prototype because of closer proximity of the electromagnet coil to the sensor.

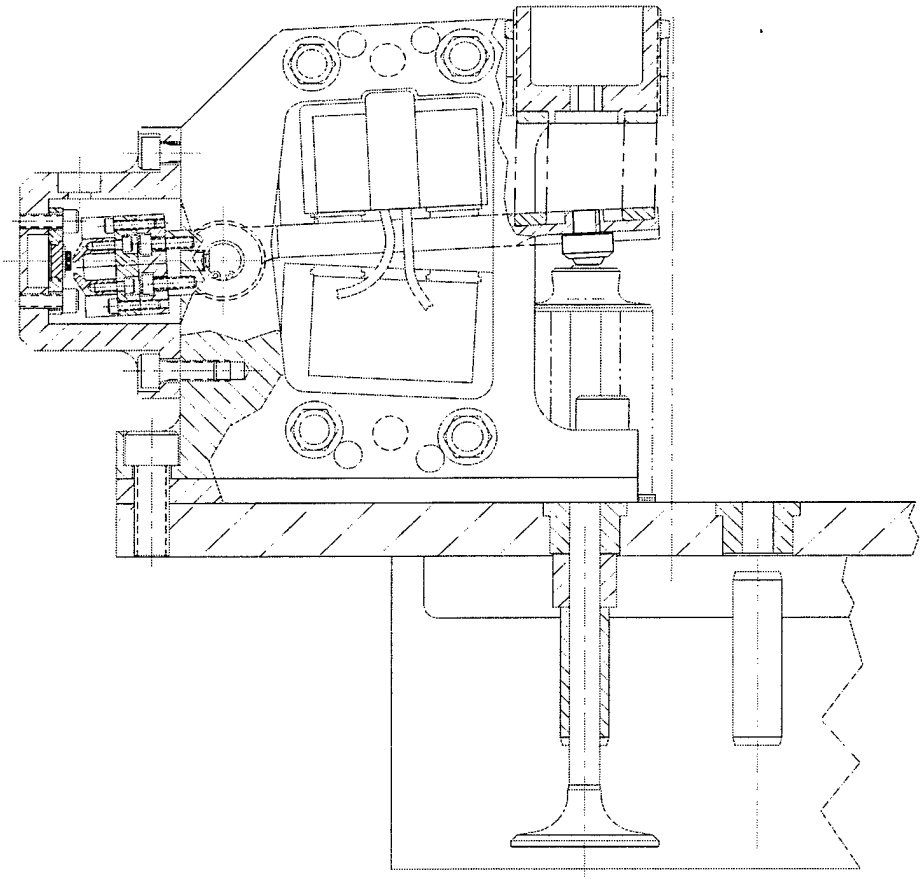

Figure 7: VORAD Actuator and Cylinder Head Layout

A VORAD electromagnet design was chosen for the Kohler engine because of good performance in previous engines, see figure 7. Size was not a consideration due to the prototype nature of this engine.

The final piece of hardware added to the system was the hall sensor which was needed in order to run the system closed loop. With the hall effect position sensor our electronics can distinguish slow armature landings from fast armature landings and adjust the current supplied to the electromagnets to control the landing velocity.

3.1 Electrical Development

The as-built system uses eight off-the-shelf current amplifiers, one for each coil. These amplifiers are rated for 50 amps peak, 25 amps continuous, with a rail voltage from 30 to 170 volts. The package size of the amplifier is about 110 mm x 185 mm x 25 mm. The amplifiers have the capability to provide positive or negative current, though are only used to provide positive current. Measured statically, the amplifier's efficiency varies from 20% to nearly 100%, with minimum efficiency during low current output (holding) and maximum efficiency during high output current (catching), which means that the amplifiers are most efficient during the highest power demands of maximum RPM and load.

Currently, the voltage rail used by the current amplifiers to energize the electromagnets is 100 volts. There are several reasons for the high rail voltage. The amount of power that must be delivered to the actuators depends on the amount of mechanical energy lost due to friction and other losses. Given that a certain amount of power is needed, it can be delivered in a current to voltage proportion set by coil impedance

$$\text{Electromagnet Power} = (\text{Coil Current}) \times (\text{Coil Voltage})$$

$$\text{Coil Impedance} = \text{Coil Voltage}/\text{Coil Current}.$$

The physical constraint for how much voltage a wire can carry is determined by the wire's insulation, and is about 300 volts for off the shelf magnet wire. The physical constraint for how much current a wire can carry is proportional to the wire's cross sectional area. The most economical and energy efficient way to carry power through a wire is using maximum voltage and minimum current, since insulation is both inexpensive and light weight, and resistive losses (current ^{2} x resistance) are minimized. The coil impedance was designed with all these factors in mind within the constraints of the available amplifiers.

3.2 Armature Position Sensing

To keep power consumption to a minimum and assure a low seating velocity of the valve, it was determined that armature position and velocity feedback were necessary as part of the control strategy. Aura's extensive experience with closed loop position servos used in the actuator line was applied to the problem, and a small, accurate, inexpensive sensing solution was found. The sensor chosen was a Hall effect sensor with an internal amplifier and temperature compensation

circuit (about 10 mm x 20 mm x 1 mm). Aura designed the magnetic circuit and sensor packaging for this application.

The VORAD prototype sensor uses samarium cobalt magnets, encapsulated in aluminum and terminated with steel pole pieces, which are mounted on the rear of the armatures. Internally temperature compensated Hall effect sensors are mounted very close to the magnets to detect change in magnetic field due to motion of the magnet. The output of the sensor is a voltage linearly proportional to armature position.

There are several sources of errors inherent to the Hall effect derived position measurement. The primary source of error results from sensor pickup of the strong magnetic fields generated by the electromagnet. Other sources of error are the hysteresis within the steel pole pieces, temperature sensitivity of the magnet, and metallic contaminants. These errors require a larger amount of power be delivered to the electromagnets to assure reliable operation.

Brief experiments utilizing the electromagnet inherent back EMF voltage as a position sensor. Preliminary results were promising. After reviewing the signal processing required to utilize the electromagnet coils as sensors, it was determined that this would require a significant amount of development effort, and the benefit of not needing an external sensor did not justify the allocation of resources.

3.3 Servo Development

The purpose of the servo is to measure armature position and velocity from the Hall sensors and adjust the power delivered to the electromagnets to minimize the power consumption and control the armature landing velocity.

Initial EVA servo development was done using analog electronics. For this program a micro-controller version was developed to add development flexibility. Two basic control approaches were built, one time based, the other position based. Both servos measured velocity and modulated the catch current turn on point, one as a function of the time elapsed after release, the other as a function of armature position. Armature position proved to be the most reliable approach. Velocity was measured as the armature transitions from seventy to eighty-five percent of travel.

For intake opening, intake closing, and exhaust closing, landing velocity is proportional to average velocity, so the present measurement scheme yields overall satisfactory operation. However, the average velocity during exhaust opening is greatly affected by residual exhaust pressure, so it is challenging to maintain a high overall transition velocity with soft landing. Therefore, soft landing is sacrificed in the exhaust opening servo to achieve optimum engine performance through fast valve transition. It is ideal to measure and control average velocity as well as landing velocity, so efforts are continuing in this area.

3.4 Measured Engine Performance

Preliminary dynamometer testing was conducted at BKM in San Diego, California. Baseline engine testing was conducted before modification of the cylinder heads for the EVA actuators. The EVA equipped engine testing was conducted over a period of three days, with roughly 16 hours of operation under full load (≈45 hours total run time). Engine performance data was collected by a Stuska Water Brake Dynamometer, the data collected included engine torque, engine horsepower, fuel consumption, air flow, barometric pressure, air temperature, oil pressure and exhaust temperature.

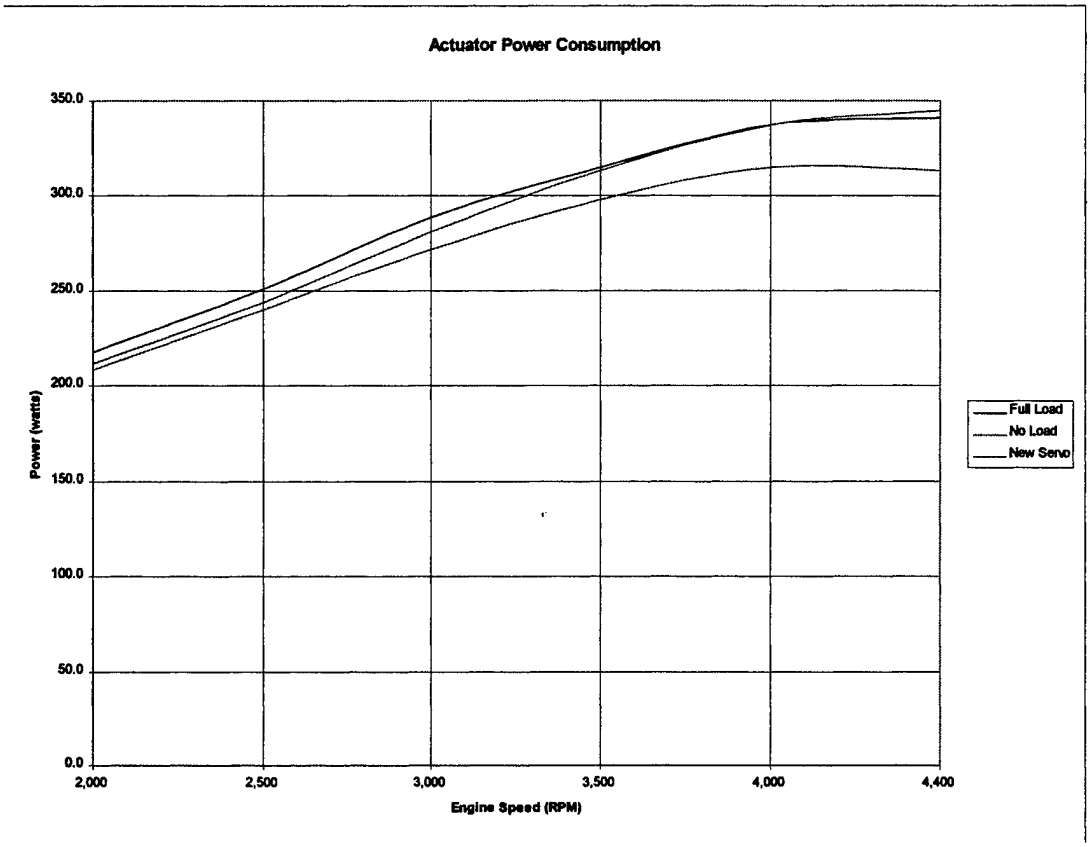

Figure 8. Actuator Power Consumption Under Full and Partial Load

Results from the EVA equipped Kohler engine, showed an increase in power between 1,200 RPM to 3,700 RPM, a net gain of ≈10%. With the increase in volumetric efficiency we observe an effective decrease in BSFC. Figures 9 and 10 are graphs which compare the EVA performance to the standard camshaft based engine.

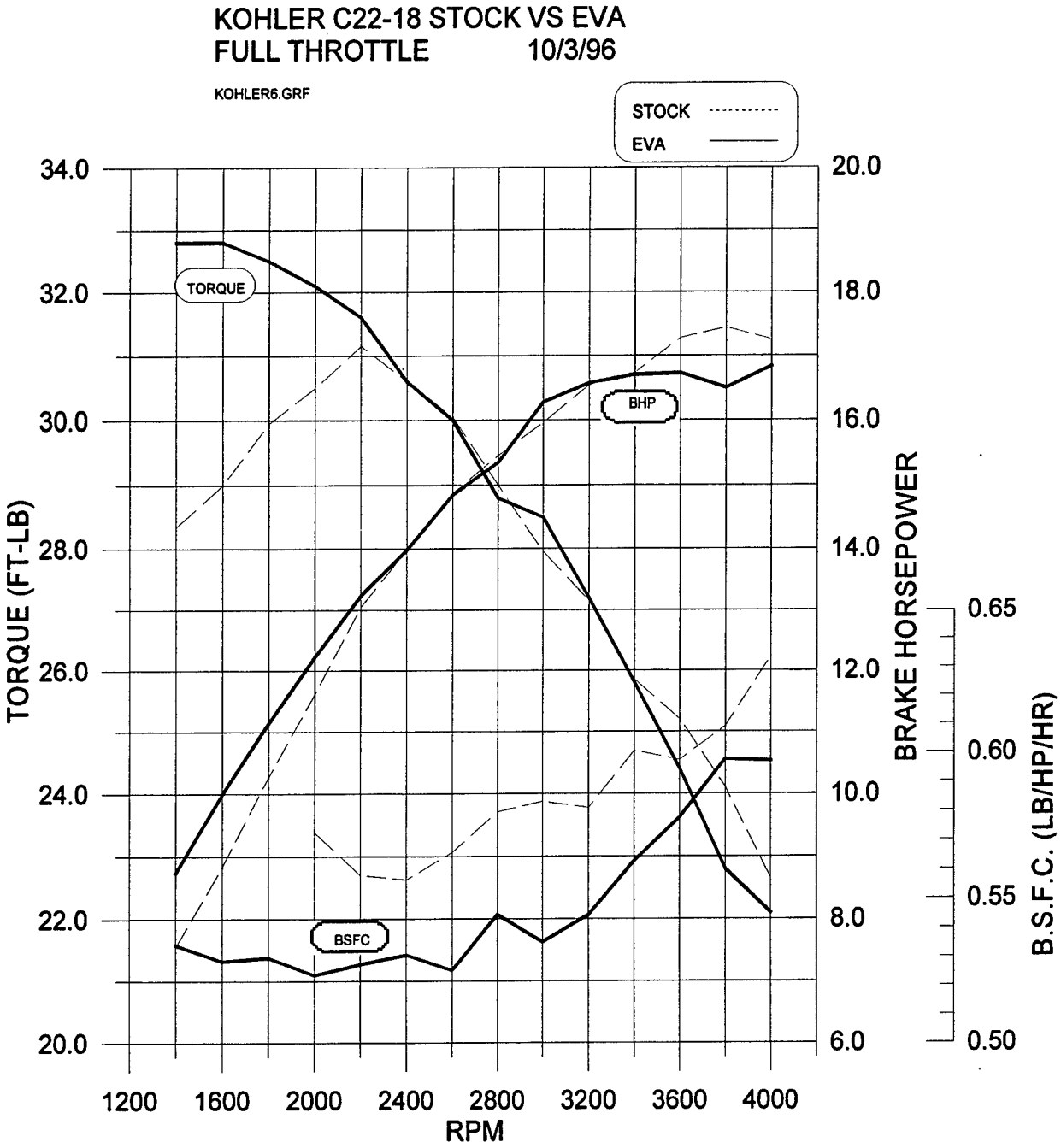

Figure 9. Engine Performance Before and After EVA retrofit.

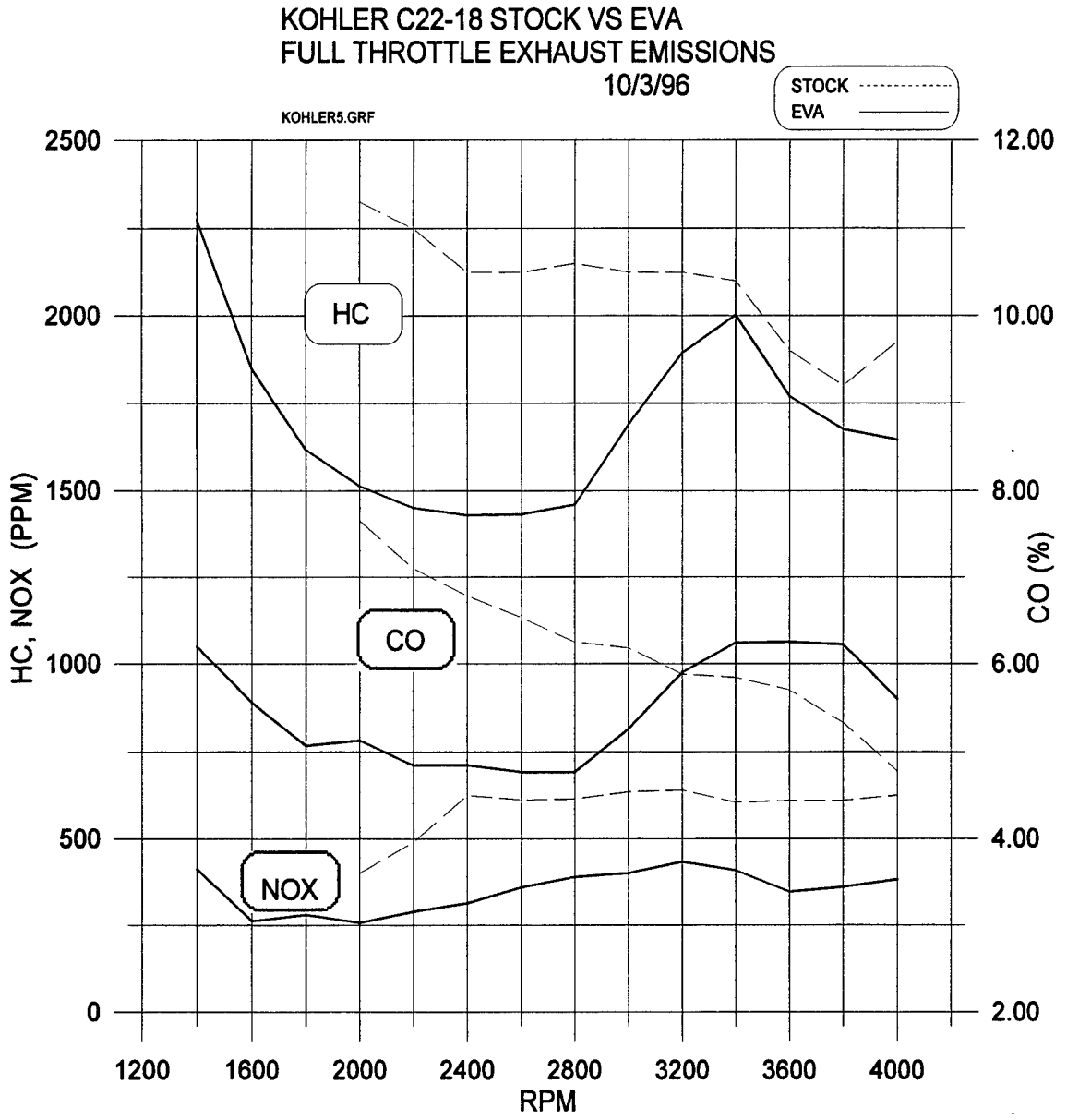

Figure 10: Pre-Catalytic Converter Emissions Before and After EVA

4.0 Detailed Analysis of Component Improvement

Reviewing the EVA engine performance shows that a benefit in horsepower from variable valve timing is realizable. However, the benefit is offset by added engine weight, size, and electrical power consumption (which must be generated from engine power). Therefore, the primary goals for an improved system are reduced weight, size and electrical power consumption. Actuator size and weight reduction are proportional. Power reduction is also tied to size reduction, though the relationship is more complicated.

Writing a simple energy balance,

EVA Power Consumption = Mechanical Power + Resistive Heating + Core Losses + Frictional Losses + Power Supply Losses

Where:

1. Mechanical power is defined as the work done against pressure forces, both on the valve head and on the armature.

2. Resistive heating is defined as the sum of all power dissipated in the electrical wires from the power supply (battery) up to and including the electromagnet coils

3. Core losses are defined as all power dissipated in the electromagnet cores and surrounding electrically conductive material due to currents induced by changing magnetic fields (eddy currents).

4. Frictional losses are defined as all losses due to friction between moving components (valve guide/valve, armature bushing, valve/armature, internal spring heating etc.).

5. Power Supply losses are defined as all losses in the conversion from mechanical to electrical power, such as alternator and power conditioning electronics.

4.1 Actuator Size and Power Reduction

Actuator size is determined from three basic constraints; transition time, opening force, and moving mass. The primary difference between intake and exhaust valves is the high opening force requirement for exhaust. Opening the exhaust valve against the residual exhaust pressure in the cylinder requires a significant amount of mechanical energy which must be stored in the open-spring and restored by the open-electromagnet. Due to substantial differences between intake and exhaust valves, they are considered separately.

The opening force necessary to overcome exhaust residual pressure is the primary factor that determines the spring rate. This force determines the electromagnet size. The open electromagnet must replace the mechanical energy absorbed by the exhaust gas. While the close electromagnet must initialize the armature from the neutral position prior to engine startup and hold the armature closed against the compressed force of the open spring. The different requirements for opening and closing electromagnets suggest using different electromagnets and offsetting the spring equilibrium position toward open.

Valve mass and transition time are the critical constraints of the intake actuator size. To move the actuator lower, the actuator size must be reduced to clear the present gap between the stock spring cup and the interface plate, reducing actuator size is both desirable and possible. The goal for the intake actuator would be to use a stock length valve, possibly drilled out to reduce weight. Since the current EVA valves are made out of titanium the valve mass is reduced almost in half.

The lower intake electromagnet force requirement reduces both the armature and electromagnet size, which further reduces moving mass. Finally, since both eddy currents and coil resistance are proportional to volume, smaller electromagnets will reduce electrical power consumption.

The current exhaust electromagnets are fairly well optimized. If we increase the coil pocket width, thus decreasing the cross section of the pole area, we could reduce the magnetic flux leakage and generate more initial opening force. The expected benefit of optimized exhaust valve actuators is approximately five percent faster transition time for exhaust open. Reducing the valve length (mass) could reduce the actuator size by up to three percent.

Both intake and exhaust actuator size could be reduced by returning to the "direct drive" approached outlined in section 2. For the rotating armature design, the spring's moment arm is twice the electromagnet's resultant force moment arm, meaning that the electromagnet must develop a force equal to twice the opening force. Using direct drive electromagnets would theoretically cut the current actuator size in half. Since the manufacture of this EVA system Aura has developed a direct drive actuator configuration that would fit this engine valve spacing.

4.2 Engine Modifications

The modifications required to make the EVA retrofit include:

1. Removal and modification of the existing cylinder heads to accept special interface plates that adapt the actuators to the cylinder head.

2. Longer custom valves, a MAP sensor to determine engine load for the valve timing look up tables.

3. Addition of a twelve tooth trigger wheel which mounts to the output (crank) shaft and is used to provide position timing to the ECU which calculates the valve timing events.

FUELS DISTRIBUTION LIST

Department of Defense

DEFENSE TECH INFO CTR 12
ATTN: DTIC OCC
8725 JOHN J KINGMAN RD
STE 0944
FT BELVOIR VA 22060-6218

ODUSD
ATTN: (L) MRM 1
PETROLEUM STAFF ANALYST
PENTAGON
WASHINGTON DC 20301-8000

ODUSD
ATTN: (ES) CI 1
400 ARMY NAVY DR
STE 206
ARLINGTON VA 22202

HQ USEUCOM
ATTN: ECJU L1J 1
UNIT 30400 BOX 1000
APO AE 09128-4209

US CINCPAC
ATTN: J422 BOX 64020 1
CAMP H M SMITH
HI 96861-4020

JOAP TSC 1
BLDG 780
NAVAL AIR STA
PENSACOLA FL 32508-5300

DIR DLA
ATTN: DLA MMSLP 1
8725 JOHN J KINGMAN RD
STE 2533
FT BELVOIR VA 22060-6221

CDR
DEFENSE FUEL SUPPLY CTR
ATTN: DFSC I (C MARTIN) 1
DFSC IT (R GRAY) 1
DFSC IQ (L OPPENHEIM) 1
8725 JOHN J KINGMAN RD
STE 2941
FT BELVOIR VA 22060-6222

DIR
DEFENSE ADV RSCH PROJ AGENCY
ATTN: ARPA/ASTO 1
3701 N FAIRFAX DR
ARLINGTON VA 22203-1714

Department of the Army

HQDA
ATTN: DALO TSE 1
DALO SM 1
500 PENTAGON
WASHINGTON DC 20310-0500

SARDA
ATTN: SARD TT 1
PENTAGON
WASHINGTON DC 20310-0103

CDR AMC
ATTN: AMCRD S 1
AMCRD E 1
AMCRD IT 1
AMCEN A 1
AMCLG M 1
AMXLS H 1
5001 EISENHOWER AVE
ALEXANDRIA VA 22333-0001

U.S. ARMY TACOM
TARDEC PETR. & WTR. BUS. AREA
ATTN AMSTA TR-R/210 (L. VILLHAHERMOSA) 10
AMSTA TR-R/210 (T. BAGWELL) 1
WARREN, MI 48397-5000

CDR ARMY TACOM
ATTN: AMSTA IM LMM 1
AMSTA IM LMB 1
AMSTA IM LMT 1
AMSTA TR NAC MS 002 1
AMSTA TR R MS 202 1
AMSTA TR D MS 201A 1
AMSTA TR M 1
AMSTA TR R MS 121 (C RAFFA) 1
AMSTA TR R MS 158 (D HERRERA) 1
AMSTA TR R MS 121 (R MUNT) 1
AMCPM ATP MS 271 1
AMSTA TR E MS 203 1
AMSTA TR K 1
AMSTA IM KP 1
AMSTA IM MM 1
AMSTA IM MT 1
AMSTA IM MC 1
AMSTA IM GTL 1
AMSTA CL NG 1
USMC LNO 1
AMCPM LAV 1
AMCPM M113 1
AMCPM CCE 1
WARREN MI 48397-5000

MOBILITY TECH CTR BELVOIR
ATTN: AMSTA RBFF (T.C. BOWEN) 1
10115 GRIDLEY RD STE 128
FT BELVOIR VA 22060-5843

PROG EXEC OFFICER
ARMORED SYS MODERNIZATION
ATTN: SFAE ASM S 1
SFAE ASM H 1
SFAE ASM AB 1
SFAE ASM BV 1
SFAE ASM CV 1
SFAE ASM AG 1
CDR TACOM
WARREN MI 48397-5000

PROG EXEC OFFICER
ARMORED SYS MODERNIZATION
ATTN: SFAE FAS AL 1
SFAE FAS PAL 1
PICATINNY ARSENAL
NJ 07806-5000

PROG EXEC OFFICER
TACTICAL WHEELED VEHICLES
ATTN: SFAE TWV TVSP 1
SFAE TWV FMTV 1
SFAE TWV PLS 1
CDR TACOM
WARREN MI 48397-5000

PROG EXEC OFFICER
ARMAMENTS
ATTN: SFAE AR HIP 1
SFAE AR TMA 1
PICATINNY ARSENAL
NJ 07806-5000

PROG MGR
UNMANNED GROUND VEH
ATTN: AMCPM UG 1
REDSTONE ARSENAL
AL 35898-8060

DIR
ARMY RSCH LAB
ATTN: AMSRL PB P 1
2800 POWDER MILL RD
ADELPHIA MD 20783-1145

VEHICLE PROPULSION DIR
ATTN: AMSRL VP (MS 77 12) 1
NASA LEWIS RSCH CTR
21000 BROOKPARK RD
CLEVELAND OH 44135

CDR AMSAA
ATTN: AMXSY CM 1
AMXSY L 1
APG MD 21005-5071

CDR ARO
ATTN: AMXRO EN (D MANN) 1
RSCH TRIANGLE PK
NC 27709-2211

CDR AEC
ATTN: SFIM AEC ECC (T ECCLES) 1
APG MD 21010-5401

CDR ARMY ATCOM
ATTN: AMSAT I WM 1
AMSAT I ME (L HEPLER) 1
AMSAT I LA (V SALISBURY) 1
AMSAT R EP (V EDWARD) 1
4300 GOODFELLOW BLVD
ST LOUIS MO 63120-1798

CDR ARMY SOLDIER SPT CMD
ATTN: SATNC US (J SIEGEL) 1
SATNC UE 1
NATICK MA 01760-5018

CDR ARMY ARDEC
ATTN: AMSTA AR EDE S 1
PICATINNY ARSENAL
NJ 07808-5000

CDR ARMY WATERVLIET ARSN
ATTN: SARWY RDD 1
WATERVLIET NY 12189

CDR APC
ATTN: SATPC L 1
SATPC Q 1
NEW CUMBERLAND PA 17070-5005

CDR ARMY LEA
ATTN: LOEA PL 1
NEW CUMBERLAND PA 17070-5007

CDR ARMY TECOM
ATTN: AMSTE TA R 1
AMSTE TC D 1
AMSTE EQ 1
APG MD 21005-5006

PROJ MGR PETROL WATER LOG
ATTN: AMCPM PWL 1
4300 GOODFELLOW BLVD
ST LOUIS MO 63120-1798

CDR
ARMY COLD REGION TEST CTR
ATTN: STECR TM 1
STECR LG 1
APO AP 96508-7850

CDR
ARMY BIOMED RSCH DEV LAB
ATTN: SGRD UBZ A 1
FT DETRICK MD 21702-5010

CDR FORSCOM
ATTN: AFLG TRS 1
FT MCPHERSON GA 30330-6000

CDR TRADOC
ATTN: ATCD SL 5 1
INGALLS RD BLDG 163
FT MONROE VA 23651-5194

CDR ARMY ARMOR CTR
ATTN: ATSB CD ML 1
ATSB TSM T 1
FT KNOX KY 40121-5000

CDR ARMY QM SCHOOL
ATTN: ATSM PWD 1
FT LEE VA 23001-5000

ARMY COMBINED ARMS SPT CMD
ATTN: ATCL MS 1
FT LEE VA 23801-6000

CDR ARMY FIELD ARTY SCH
ATTN: ATSF CD 1
FT SILL OK 73503

CDR ARMY TRANS SCHOOL
ATTN: ATSP CD MS 1
FT EUSTIS VA 23604-5000

CDR ARMY INF SCHOOL
ATTN: ATSH CD 1
ATSH AT 1
FT BENNING GA 31905-5000

CDR ARMY AVIA CTR
ATTN: ATZQ DOL M 1
ATZQ DI 1
FT RUCKER AL 36362-5115

CDR ARMY ENGR SCHOOL
ATTN: ATSE CD 1
FT LEONARD WOOD
MO 65473-5000

CDR 49TH QM GROUP
ATTN: AFFL GC 1
FT LEE VA 23801-5119

CDR ARMY ORDN CTR
ATTN: ATSL CD CS 1
APG MD 21005

CDR ARMY SAFETY CTR
ATTN: CSSC PMG 1
CSSC SPS 1
FT RUCKER AL 36362-5363

CDR ARMY ABERDEEN TEST CTR
ATTN: STEAC EN 1
STEAC LI 1
STEAC AE 1
STEAC AA 1
APG MD 21005-5059

CDR ARMY YPG
ATTN: STEYP MT TL M 1
YUMA AZ 85365-9130

CDR ARMY CERL
ATTN: CECER EN 1
P O BOX 9005
CHAMPAIGN IL 61826-9005

DIR 1
AMC FAST PROGRAM
10101 GRIDLEY RD STE 104
FT BELVOIR VA 22060-5818

CDR I CORPS AND FT LEWIS
ATTN: AFZH CSS 1
FT LEWIS WA 98433-5000

CDR
RED RIVER ARMY DEPOT
ATTN: SDSRR M 1
SDSRR Q 1
TEXARKANA TX 75501-5000

PS MAGAZINE DIV
ATTN: AMXLS PS 1
DIR LOGSA
REDSTONE ARSENAL AL 35898-7466

CDR 6TH ID (L)
ATTN: APUR LG M 1
1060 GAFFNEY RD
FT WAINWRIGHT AK 99703

Department of the Navy

OFC CHIEF NAVAL OPER
ATTN: DR A ROBERTS (N420) 1
2000 NAVY PENTAGON
WASHINGTON DC 20350-2000

CDR
NAVAL SEA SYSTEMS CMD
ATTN: SEA 03M3 1
2531 JEFFERSON DAVIS HWY
ARLINGTON VA 22242-5160

CDR
NAVAL SURFACE WARFARE CTR
ATTN: CODE 63 1
CODE 632 1
CODE 859 1
3A LEGGETT CIRCLE
ANNAPOLIS MD 21402-5067

CDR
NAVAL RSCH LABORATORY
ATTN: CODE 6181 1
WASHINGTON DC 20375-5342

CDR
NAVAL AIR WARFARE CTR
ATTN: CODE PE33 AJD 1
P O BOX 7176
TRENTON NJ 08628-0176

CDR 1
NAVAL PETROLEUM OFFICE
8725 JOHN J KINGMAN RD
STE 3719
FT BELVOIR VA 22060-6224

CDR
NAVAL AIR SYSTEMS CMD
ATTN: AIR 4.4.5 (D MEARNS) 1
1421 JEFFERSON DAVIS HWY
ARLINGTON VA 22243-5360

Department of the Navy/U.S. Marine Corps

HQ USMC
ATTN: LPP 1
WASHINGTON DC 20380-0001

PROG MGR COMBAT SER SPT 1
MARINE CORPS SYS CMD
2033 BARNETT AVE STE 315
QUANTICO VA 22134-5080

PROG MGR GROUND WEAPONS 1
MARINE CORPS SYS CMD
2033 BARNETT AVE
QUANTICO VA 22134-5080

PROG MGR ENGR SYS 1
MARINE CORPS SYS CMD
2033 BARNETT AVE
QUANTICO VA 22134-5080

CDR
MARINE CORPS SYS CMD
ATTN: SSE 1
2030 BARNETT AVE STE 315
QUANTICO VA 22134-5010

CDR
BLOUNT ISLAND CMD
ATTN: CODE 922/1 1
5880 CHANNEL VIEW BLVD
JACKSONVILLE FL 32226-3404

CDR
MARINE CORPS LOGISTICS BA
ATTN: CODE 837 1
814 RADFORD BLVD
ALBANY GA 31704-1128

CDR 1
2ND MARINE DIV
PSC BOX 20090
CAMP LEJEUNNE
NC 28542-0090

CDR 1
1ST MARINE DIV
CAMP PENDLETON
CA 92055-5702

CDR 1
FMFPAC G4
BOX 64118
CAMP H M SMITH
HI 96861-4118

Department of the Air Force

HQ USAF/LGSF
ATTN: FUELS POLICY 1
1030 AIR FORCE PENTAGON
WASHINGTON DC 20330-1030

HQ USAF/LGTV
ATTN: VEH EQUIP/FACILITY 1
1030 AIR FORCE PENTAGON
WASHINGTON DC 20330-1030

AIR FORCE WRIGHT LAB
ATTN: WL/POS 1
WL/POSF 1
1790 LOOP RD N
WRIGHT PATTERSON AFB
OH 45433-7103

AIR FORCE MEEP MGMT OFC 1
OL ZC AFMC LSO/LOT PM
201 BISCAYNE DR
BLDG 613 STE 2
ENGLIN AFB FL 32542-5303

SA ALC/SFT 1
1014 BILLY MITCHELL BLVD STE 1
KELLY AFB TX 78241-5603

SA ALC/LDPG
ATTN: D ELLIOTT 1
580 PERRIN BLDG 329
KELLY AFB TX 78241-6439

WR ALC/LVRS 1
225 OCMULGEE CT
ROBINS AFB
GA 31098-1647

Other Federal Agencies

NASA
LEWIS RESEARCH CENTER 1
CLEVELAND OH 44135

RAYMOND P. ANDERSON, PH.D., MANAGER 1
FUELS & ENGINE TESTING
BDM-OKLAHOMA, INC.
220 N. VIRGINIA
BARTLESVILLE OK 74003

DOT
FAA
AWS 110 1
800 INDEPENDENCE AVE SW
WASHINGTON DC 20590

DOE
CE 151 (MR RUSSELL) 1
1000 INDEPENDENCE AVE SW
WASHINGTON DC 20585

EPA
AIR POLLUTION CONTROL 1
2565 PLYMOUTH RD
ANN ARBOR MI 48105